Operational Effectiveness of Hydrofoils for Littoral Craft: Investigating the Potential of Hydrofoils for High-Speed Daughter Craft in Amphibious Operations

R.M. Zwinkels,[1,*] J.L. Gelling,[1] R. Kalisvaart,[2] L.F. Minerva,[3] and A.A. Kana[1]

[1] *Department of Maritime and Transport Technology, Delft University of Technology, Delft, The Netherlands*
[2] *De Haas Maassluis B.V., Maassluis, The Netherlands*
[3] *Maritime Research Institute Netherlands (MARIN), Wageningen, The Netherlands*

[*] *roan.zwinkels@hotmail.com*

Abstract: This study explores the use of submerged hydrofoil systems for landing craft, with the goal of evaluating its operational effectiveness. Using a systems engineering approach, various submerged hydrofoil configurations and propulsion systems are evaluated. A design method is developed which uses iterative parametric modelling and assessment of the craft's dynamic equilibrium across its full speed range. The resulting designs are then compared to a planing benchmark vessel. The findings show a resistance reduction of 35% at cruise speeds, leading to a 50% increase in range. Seakeeping analysis of a submerged hydrofoil configuration also demonstrates that hydrofoils can increase the sustained speed in waves and effectively reduce peak vertical accelerations. The results highlight that significant gains can be made with respect to range, sustained speed, and safety, which exemplifies the potential of hydrofoil system integration despite added design complexity.

Keywords: Daughter craft, Hydrofoil, Operational effectiveness, Preliminary design, Ship design, Littoral

1. Introduction

Landing craft are essential for the rapid deployment of personnel, vehicles, and equipment from ship to shore. These craft are launched from mother ships such as the Landing Platform Dock (LPD) and Joint logistic Support Ship (JSS) of the Royal Netherlands Navy (RNLN). Due to the current increase in threats from shore however, mother ships will tend to extend their distance from the coast in the future. This implies that their daughter (landing) craft have to traverse a larger distance to the shoreline. In 2019, the Dutch commander of the naval forces (CZSK) introduced the Future Littoral Operating Concept (FLitOC), developed in close cooperation with the United States and the United Kingdom (Strijbosch, 2019). This new concept entails an increase in transit distance from around 10 nm to 40 nm. Going further offshore shifts risk from the mother ship to the daughter craft, which have to face worse sea conditions as a smaller and more exposed vessel. As a result, even greater emphasis is placed on the seakeeping, speed, and range of new landing craft designs. The main organisational changes of the new amphibious doctrine of the RNLN are summarised in Table 1.

Table 1: The main organisational changes of the updated amphibious doctrine of the RNLN based on letters to parliament (Kamp, 2021; van der Maat, 2023, 2024)

Current doctrine (2025)	**New doctrine (2035)**
Few large mother ships	More smaller mother ships
Mother ships at small distance of shore ($\approx$ 10 nm)	Mother ships at large distance of shore ($\approx$ 40 nm)
Multiple waves of marines	Simultaneous deployment
Limited deployment areas	Multiple spaced out deployment areas

Currently, the primary daughter craft used in amphibious operations are the Landing Craft Vehicle Personnel (LCVP) and the Landing Craft Utility (LCU). The LCVP's main purpose is the transfer of personnel and light vehicles, while the larger LCU is intended for heavy vehicle transport and associated personnel. The Netherlands Ministry of Defence (NLMOD) has stated its intentions to replace the LCVP within the coming five years (van der Maat, 2023), with two new types of craft: the Littoral Assault Craft (LAC) and Littoral Craft Mobility (LCM). Whereas the LAC will take over most of the personnel transfer of the LCVP, the Littoral Craft Mobility (LCM) is intended to take over the light vehicle transport. Of these craft, the LAC will be introduced first and will be the primary focus of this study.

The LCVP (shown in Fig. 1) is characterised by a flat bottom hull and large bow ramp. Apart from waterjet propulsion integration, the design has remained mostly unchanged since World War II. Van den Bosch (1970) notes

that, although low deadrise hulls like the LCVP have relatively low calm water resistance, it is generally accompanied by bad seakeeping performance. A potential candidate for the LAC is the CB90 (see Fig. 2), which has a more V-shaped hull and a smaller bow ramp designed exclusively for personnel embarkation and disembarkation. However, it is still an older design, introduced in the 1990s, which is primarily intended for sheltered shallow water regions such as rivers or fjords (Saab, 2021). It is therefore of interest to investigate how the operational effectiveness can be increased further for the updated requirements of the NLMOD.

Fig. 1: Landing Craft Vehicle Personnel (LCVP mkV(c)) (Netherlands Ministry of Defense, n.d.)

Fig. 2: Swedish Combat Boat 90 (Stridsbåt 90, CB 90) in the port of Gothenburg (Ardon, 2008)

In the design of naval vessels, the measurement of operational effectiveness is a point of contention (Stam, 2025; Streng et al., 2022). Effectiveness of a cargo ship is often quantified in capacity and speed for example, resulting in efficiency measurements such as transport efficiency or the Energy Efficiency Design Index (EEDI). The effectiveness of a naval vessel is not solely assessed on these efficiencies and is for a greater part quantified by its other capabilities. Therefore, this study aims to provide a qualitative assessment of the operational effectiveness of the application of hydrofoils by the use of several distinctive Measures of Effectiveness (MoEs). Kossiakoff et al. (2020) describes MoEs as "a qualitative or quantitative metric of a system's overall performance that indicates the degree to which it achieves it objectives under specified conditions". A MoE therefore refers to the system as a whole. By investigation of current NLMOD requirements for an LAC (Netherlands Ministry of Defence, 2023), and a user interview with the Royal Netherlands Marine Corps (RNLMC), the design drivers and MoEs of Table 13 have been derived.

As daughter craft are launched from the mother ship's welldeck or davits, new designs have to account for strict dimensional requirements. These requirements, and the required payload are listed in Table 2. Due to these constraints, increasing seakeeping capabilities and range is difficult to achieve with conventional methods. Concepts previously applied to improve seakeeping of high-speed craft are build upon the principle of increasing the size of the vessel to reduce maximum vertical accelerations (Gelling & Keuning, 2011). Increasing the deadrise angle of the vessel can also improve seakeeping performance, but complicates the landing procedure (Keuning et al., 1992).

Table 2: Summary of additional main requirements of a future LAC design

Parameter	**Value**	**Reasoning**
L_{oa}	16 m (max)	L_{oa} of CB90 (Davits)
B	4.27 m (max)	B of LCVP (Davits)
T	0.86 m (max)	Requirement - same as CB90
Payload	16 passengers (4.5 t)	Requirement
Crew	3	Requirement
Bow hatch and ramp	-	Requirement

Seakeeping can also be increased by applying Advanced Marine Vehicle (AMV) hull concepts (McKesson, 2014). By evaluating different AMV concepts it becomes clear that hydrofoils offer the greatest potential in achieving the greater demands of the NLMOD. This is attributed to:

- the highest transport efficiency at the required speeds of any AMV, which can increase range as a result (van Oossanen, 1983);
- the high sustained speed through rough seas (Johnston, 1985);
- the low vertical accelerations at high speed to reduce fatigue and physical strain of crew (Johnston, 1985);
- the load carrying ability being sufficient for passenger transport (McKesson, 2014);
- the successful prior application of retraction systems for hydrofoils (Yun & Bliault, 2014);
- the reduced importance of economics for the navy, provided sufficient gains in other performance aspects can be realised.

2. Hydrofoil systems and propulsion

Hydrofoils have recently seen renewed interest for their energy-saving potential. Modern designs also benefit from advancements in composite materials and control systems (Godø, 2024). Fig. 3 presents the design space of a hydrofoil implementation of an LAC. It highlights that the design space occupies a middle ground between the traditional focus on hydrofoils for military or ferry use and the recent enthusiasm in hydrofoils, primarily for leisure boating. This suggests that such an implementation can blend elements from both the classic and modern approaches.

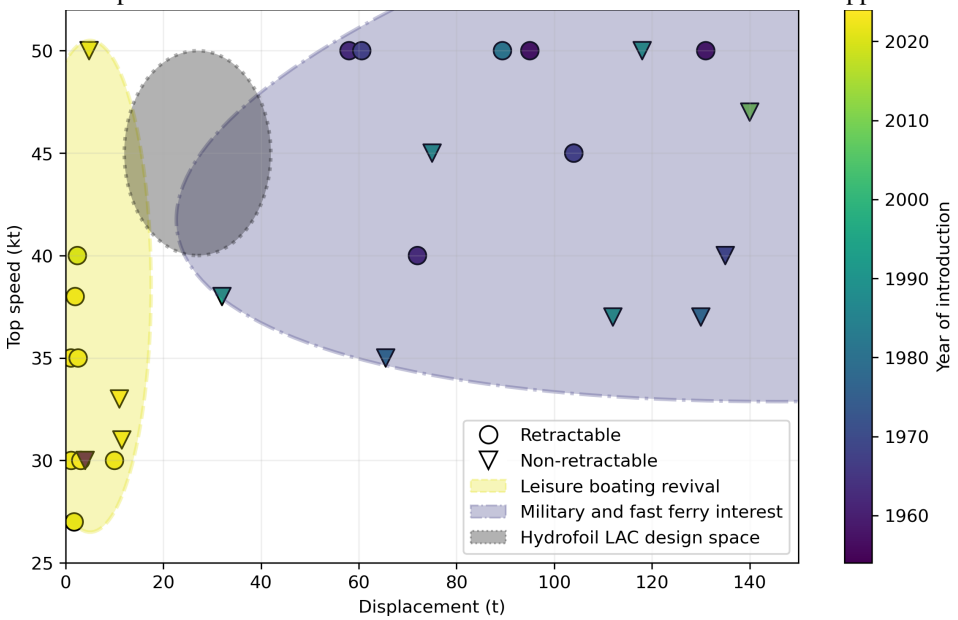

Fig. 3: Design space of a future hydrofoil LAC craft (Artemis, 2024; Candela, 2024a; Edorado, 2024; Emirates Team New Zealand, 2022; Enata, 2024; German Maritime Museum, 2024; James, 2024; Mantaray, 2024; Navier, 2024; SEAir solutions, 2024; Tyde, 2024; Vessev, 2024; Yun & Bliault, 2014)

Table 3 lists the functional requirements of a viable retractable hydrofoil system for an LAC design. The requirements are based on the main concerns of the RNLMC, expressed in an user interview. The small draught requirement (HF REQ 1) yields from the requirement that the craft is beached for personnel transfer. The second requirement (HF REQ 2) expresses the minimum operability of the system demanded by the RNLMC. Other requirements are regarding the redundancy and safety of the system. Although the fifth requirement (HF REQ 5) is deemed out of the scope of this study, it is important to note that this is a feature applied in retractable hydrofoil systems (Hosseini, 2024). An additional mitigating system can be a collision-avoidance system, utilising sensors to identify and detect obstacles in advance. Hydrofoil craft manufacturers publicise to have such systems in place, but report little about their effectiveness (Artemis, 2024; Hosseini, 2024).

Table 3: Retractable hydrofoil system functional requirements

No.	Requirement
HF REQ 1	The hydrofoil system SHALL not extend further than the maximum draught of the craft (0.86 m) in retracted mode
HF REQ 2	The hydrofoil system SHALL be deployed in conditions up to and including sea state 3 ($H_{1/3} = 1.25$ m)
HF REQ 3	The hydrofoil system SHALL have measures to remain in operation after encountering floating debris
HF REQ 4	The hydrofoil system SHALL have redundancy in its transmission system to remain manoeuvrable after a critical failure of one of the foil systems (per strut)
HF REQ 5	The hydrofoil system SHALL have designated shear-off points in the case of collision with a large object or running aground to avoid damage to the hull

2.1. Retraction

Hydrofoil retraction is typically implemented using electromechanical or hydraulic systems, with the retraction direction being vertical, lateral, or astern, depending on foil configuration (see Table 5) (Johnston, 1985; Yun & Bliault, 2014). Although hydraulic systems are generally heavier and require more power, they offer better scalability and are advantageous when existing hydraulic infrastructure is present, such as for foil actuation (Lundin & Eriksson,

2021). The retraction mechanism itself may account for as little as 1.8% of the total vessel weight (Lundin & Eriksson, 2021). The total weight fraction of older retractable hydrofoil systems, including the structural weight of foils and struts, ranged between 10-15% (Johnston, 1985). These systems were constructed from high-strength steel, aluminium or titanium (Johnston, 1985). Modern use of carbon composites can significantly reduce the structural weight, with recent findings indicating the combined strut and foil structural weight as low as 1-5% (Godø et al., 2024).

2.2. *Propulsor*

For the intended speed range of a future LAC design ($>$ 30 kt), waterjets and propellers can be applied (Keuning & Ligtelijn, 2017). The propellers at this design speed are of the trans- or supercavitating type. Both waterjets and propellers have been successfully applied in prior hydrofoil designs (Yun & Bliault, 2014). Although propellers in themselves are relatively simple, integration into a hydrofoil design requires a complex transmission system. With the use of waterjets, heavily-loaded gears and long transmission shafts are eliminated, and the number of moving parts is reduced. This simplicity, however, comes with a considerable increase in required power. Johnston (1985) considers an increase of required installed power compared to propellers of around 20% at 50 kt to approximately 100% at common take-off speeds (20-30 kt). The lower efficiency of high-speed propulsors at lower speeds can pose a risk, as the hump resistance can become the defining factor for the required propulsion power (Faltinsen, 2005).

2.3. *Transmission*

Propulsion transmission for hydrofoil craft is typically integrated in the hydrofoil struts. Table 4 lists estimated performance of several transmission concepts for retractable hydrofoils, derived from literature and supplier data. The geared drive system serves as the benchmark transmission system, as seen in the CB90 and other waterjet applications. "Long shafts" refer to shafts that travel through the hydrofoil struts. Shaft and gearbox losses follow recommendations by Klein Woud and Stapersma (2002). Power electronics losses, incurred by converters, inverters and motor controllers, are estimated at 4% for DC grids based on supplier data (ABB, 2022). Electric motor losses are estimated at 3%, based on ABB industrial motors (2023), whereas the estimates for hydraulic systems of the hydrostatic drive are values taken from Dymarski and Skorek (2006). Furthermore, the homokinetic joint losses of 2% are based on a 15° operating angle from Cirelli et al. (2021).

Table 4: Transmission performance estimates with the losses per component, the total transmission efficiency (η_{trm}) and number of components n.

Geared drive		**Homokinetic**		**Z-drive**		**Electric L-drive**		**Electric podded**		**Hydrostatic**	
Comp.	Loss	Comp.	Loss	Comp.	Loss	Comp.	Loss	Comp.	Loss	Comp.	Loss
Gearbox	1.0%	Gearbox	1.0%	2 Gearboxes	1.0%	Power elec.	4.0%	Power elec.	4.0%	Hydraulic pump	9.0%
2 Shafts	0.5%	Shaft	0.5%	2 Shafts	0.5%	Electric motor	3.0%	Electric motor	3.0%	Hydraulic motor	6.0%
		Long shaft	1.0%	Long shaft	1.0%	Gearbox	1.0%	(Reduced η_o)[1]	5.0%	Gearbox	1.0%
		Joint	2.0%			Shaft	0.5%			Shaft	0.5%
		(Prop. angle)	3.5%			Long shaft	1.0%				
η_{trm}	98%	96% (92%)		96%[2]		91%		93% (88%)		84%	
n	3	4		5		5		2		4	

Though not yet applied in hydrofoil craft, a homokinetic transmission is found in sailing yachts (Bieker Boats, 2012; Ship Motion Group, 2024). A homokinetic joint (also called a constant-velocity joint) can lower the propeller shaft to the required inclination angle. This allows for relatively simple propulsion system, but remains challenging to implement due to the positioning of the prime mover.

Z-drive transmissions were used in retractable designs for early military hydrofoil craft (Frauenberger, 1982). However, reliability issues with this gear transmission system has proved to make successful implementation difficult (Johnston, 1985).

L-drive transmission in combination with vertical retraction has seen use in recent battery-electric hydrofoil craft (Navier, 2024; Vessev, 2024). For this configuration an electrical motor is integrated within the top of the strut. As a result, the only tether to the hull is the electrical connection, with possibly cooling as well.

Electrical transmission in combination with podded propellers also has seen recent applications for battery-electric hydrofoil craft (Artemis, 2024; Candela, 2024b). With the use of a podded electrical motor, gear transmission through the strut is eliminated and the strut design is simplified. However, the increased pod size to house the electrical motor will increase drag and limit viable motor power. Furthermore, these solutions are specifically designed for their intended hydrofoil design.

[1] Increased pod drag is taken into account for η_o and accounts for around 5% of power loss (Grevink, 2022; Mewis, 2002)

[2] The Grumman (currently Northrop Grumman) company claimed an equal efficiency of 96% for the Z-drive transmission of the Shimrit class hydrofoil vessel (Peek & Bauer, 1981)

Hydrostatic transmission with hydraulic systems is also applied for retractable hydrofoil craft (Enata, 2024). Using hydraulics, flexibility in the hydrofoil retraction is achieved without the need for extensive electrical systems, however, this is substituted with an inefficient hydraulic transmission, which may be just as heavy.

2.4. *Prime mover*

The power density of prime movers is one of the primary concerns for the design of high-speed craft due to their increased weight sensitivity (McKesson, 2014). The prime movers of current hydrofoil craft are primarily high-speed 4-stroke engines and marinised gas turbines, with the exception of battery-electric designs. Fig. 4 visualises the development of weight over power of several prime mover types.

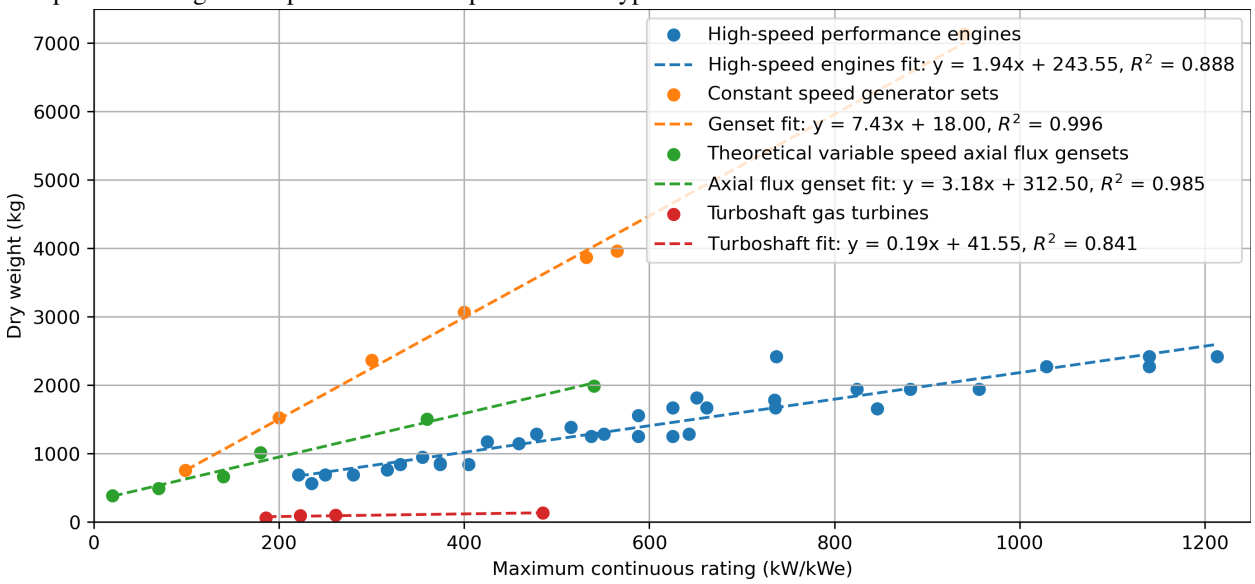

Fig. 4: Development of prime mover weight over power based on published manufacturer data (Caterpillar, 2024; Hydrosta, 2024; Man Rollo, 2024; Rolls-Royce, 2024; Scania, 2025; Volvo Penta, 2025; Yanmar, 2025)

The lightest prime movers found within the required power domain of a future LAC design is the gas turbine. Although marinised gas turbines generally start from a capacity of 3 MW (Klein Woud & Stapersma, 2002), smaller gas turbines can be found in the helicopter industry and are of the turboshaft type (Rolls-Royce, 2024). The main drawback of using gas turbines is their lower efficiency compared to combustion engines. Gas turbines have an engine efficiency (η_e) between 25 and 30%, whereas high-speed combustion engines have an efficiency (η_e) around 40%. Prior design studies have shown that although gas turbines can halve the weight fraction of propulsion machinery, this is mostly negated by the increased fuel capacity requirement due to the reduced engine efficiency (η_e), but this depends on the range requirement (Hoerner et al., 1954; Johnston, 1985).

High-speed engines, in particular V-type engines, can still offer a high power density at a higher efficiency compared to gas turbines. Due to its simplicity, maintainability and reliability, it remains the current prime mover of choice for smaller high-speed craft (Yun & Bliault, 2014). The high-speed engines of Fig. 4 are rated for a minimum of 600 hours per year, as is requested by the NLMOD. Ratings differ per engine manufacturer, but this would generally fall within the lightest load factor and the highest available rating. As a result, this is the maximum power that can be delivered by these engine blocks for commercial applications and will be the highest power-to-weight ratio available for combustion engines of this category.

Diesel-electric propulsion can facilitate less complex transmission to foilborne propulsors and offer flexibility in the placement of onboard systems. Unfortunately, employing generator sets as a prime mover in a traditional sense with constant speed generators in an AC-grid will increase the mass of prime movers drastically, as is shown by Fig. 4. Published manufacturer data of these generators are rated for continuous use and are limited in engine speed to produce a stable alternating current. To improve the power-to-weight and volume-to-weight ratio, variable speed generator sets in combination with a DC-grid architecture can be applied (Kim & Jeon, 2022; Kyunghwa Kim & Chun, 2018). This provides flexibility in the engine rating and rotational speed. An even lower weight can be achieved by employing axial-flux electrical machines (Hydrosta, 2024). Fig. 4 therefore also provides the weight development of a theoretical variable speed generator set, based on data from high-speed engines and axial flux genset conversions.

2.5. *Configuration comparison*

Table 5 shows a relative decision matrix of hydrofoil systems derived from investigation of foil configurations. The decision matrix evaluates different foil configurations based on the Pugh method (Pugh, 1991). The Pugh method is

a qualitative method to rank multi-dimensional options of an option set to a reference design. The reference option, in this case, is a planing boat and alternatives can be be better or worse on a scale of -3 to 3. Although the list of criteria options and its grading remains arbitrary, this method allows for a direct comparison and an initial selection of design options can be made. The scores in this matrix are not tallied for a total score, as the weighting of each design consideration is inherently subjective. Instead, it provides a qualitative overview of design options.

Table 5: Relative decision matrix for retractable foil configurations using the Pugh method (Pugh, 1991)

Configuration of main foil	**Planing**	**Submerged split conventional**	**Submerged non-split conventional**	**Surface-piercing split conventional**	**Submerged split canard**	**Submerged non-split canard**
Lift efficiency	0	2	3	1	2	3
Seakeeping	0	2	2	1	3	3
Manoeuvrability	0	1	1	-2	1	1
Foil complexity	0	-2	-3	-1	-2	-3
Propulsion vulnerability	0	-1	-1	-1	-2	-3
Generally applied transmission	Geared drive Waterjet	Z-drive	Electric L-drive Electric Podded	Electric L-drive Hydrostatic	Electric L-drive Waterjet	Electric L-drive Waterjet
Main foil retraction direction	-	Lateral	Vertical	Lateral	Lateral	Vertical Astern
Maximum propulsion efficiency $\eta_e \cdot \eta_{trm} \cdot \eta_D$	0.28 0.41*0.98*0.70	0.26 0.41*0.96*0.65	0.24 0.40*0.91*0.65	0.24 0.40*0.91*0.65	0.24 0.40*0.91*0.65	0.24 0.40*0.91*0.65

The surface-piercing option's decreased complexity comes at the cost of lift efficiency, seakeeping and manoeuvrability. Surface-piercing hydrofoils experience significantly less wave excitation compared to high-speed displacement or planing ships of similar size. On the contrary, the requirement for the foils to balance wave-induced forces, along with the geometric constraints of practical designs, limits the acceptable sea states for high-speed operation (Johnston, 1985). Surface-piercing hydrofoils are also less efficient than their submerged counterparts due to the increased water-air interaction and because the foils are located near the free-surface, where the lift of the foils decreases (van Walree, 1999). Furthermore, the lack of active roll control makes banked turns impossible and reduces manoeuvrability (Faltinsen, 2005).

Between submerged foil systems, less significant differences can be observed. Still, a canard configuration can offer better seakeeping due to reduced possibility of foil broaching (Johnston, 1985), whereas a conventional configuration can have better lift efficiency, due to the main front foil operating without any wake (Mørch, 1992). The differentiation between submerged options has a more direct implication for the possible propulsion methods. For example, waterjets are only applied in combination with a canard configuration due to its lift distribution and ability to let struts act as a water inlet.

To achieve redundancy in the propulsion system (following HF REQ 4), it must be split into two independent propulsion lines. This configuration positions the propulsors on either side of the vessel rather than placing a single propulsor along the centreline. An added benefit of this arrangement is that the propulsion system can be retracted higher than the vessel's keel, potentially allowing propeller systems to provide thrust even when retracted. This can work similarly to a sterndrive propulsion system. Furthermore, using two propulsion lines helps manage torque demands, preventing the excessive torque that a single propulsion line requires in a high-speed vessel. Additionally, this setup enables differential steering capability.

In a non-split canard configuration, the propulsion system is integrated with the main aft foil, so any failure of the foil endangers the entire propulsion system, making it not compliant with the hydrofoil requirements (HF REQ 4). While a split canard setup offers redundancy by splitting the system over two foils, it remains more vulnerable than the conventional configuration. A conventional configuration encounters obstacles first with its front foils and struts, offering some protection of the aft foil and propulsion system. Furthermore, a potential collision avoidance system may be able to detect these objects to react in a mitigating manner.

Based on the requirement that the foil system has to remain deployable in sea state 3 (HF REQ 2) and that 'lift efficiency' and 'seakeeping' encapsulate the design drivers (Table 13), submerged hydrofoils are selected as a foil design for further investigation. Furthermore, a conventional configuration is preferred over the canard configuration due to the propulsion vulnerability considerations. The resulting foil configuration is visualised in Section 3.4 and is also known as a π fore and split-T aft configuration. To facilitate the retraction of the front foil, a slot in the hull is necessary to make a hydrodynamically efficient hull in a retracted mode. Recent hydrofoil craft designs use a similar approach (Candela, 2024b; Vessev, 2024).

3. Design method

The design of a hydrofoil craft can be evaluated under the condition of a complete dynamic equilibrium, defined as the balance of forces and moments at each vessel speed (van Walree, 1999). Achieving this dynamic equilibrium yields

the total force in the forward direction, which defines the resistance R. Fig. 5 provides a simplified illustration of this situation. The submerged hull generates both hydrodynamic and hydrostatic forces (N) while also contributing to resistance (R). Simultaneously, the foils generate a lifting force (L), which is not perfectly aligned with the displacement weight (Δ), thereby adding a component to the resistance (R). To maintain motion, the total drag must be counteracted by the thrust (T) produced by the propulsor. These force vector directions are defined by the pitch/trim angle (τ), flap or incidence angle (δ/α) and the shaft inclination angle (ε). Consequently, the primary factors influencing resistance are:

- Weight of the vessel
- Hull Design
- Foil Design
- Foil actuation system and the maximum angle of attack
- Propulsor inclination angle

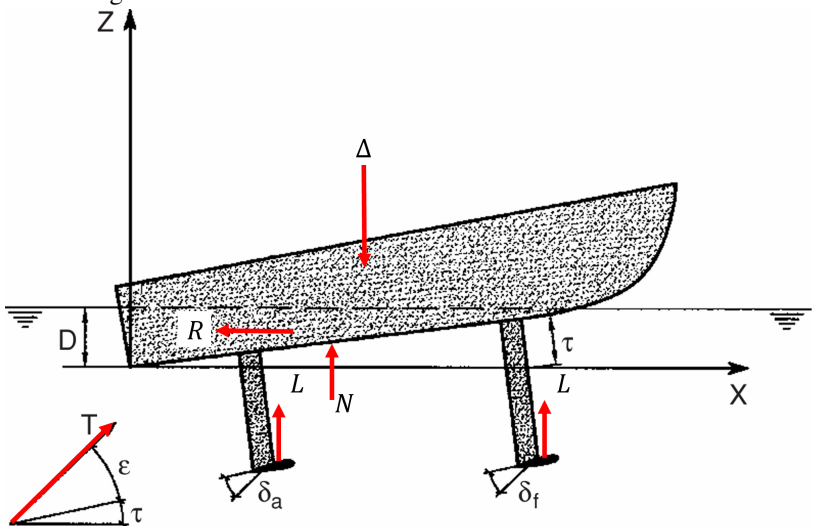

Fig. 5: Axis system for dynamic equilibrium equations, adapted from Faltinsen (2005) to show force vectors, originally from Van Walree (1999)

3.1. Top-level overview

Fig. 6 depicts the design workflow applied to the design of a hydrofoil LAC. Based on an initial lift requirement, the Foil Design JIP tool is used to explore the design space for the foils' main characteristics. The Foil Design JIP tool of the Maritime Research Institute Netherlands (MARIN) is a data-driven prediction model of lift and drag of a horizontal foil in a T-foil configuration, excluding the effects of a vertical strut. A more comprehensive description is provided by Minerva et al. (2024). Additionally, this total foiling estimate is used to iteratively evaluate the design's weight estimation and the effect on the foil design. This serves as first displacement estimate for the following step in the design process. During this part, foil interaction effects are neglected as this is a limitation of the Foil Design JIP tool.

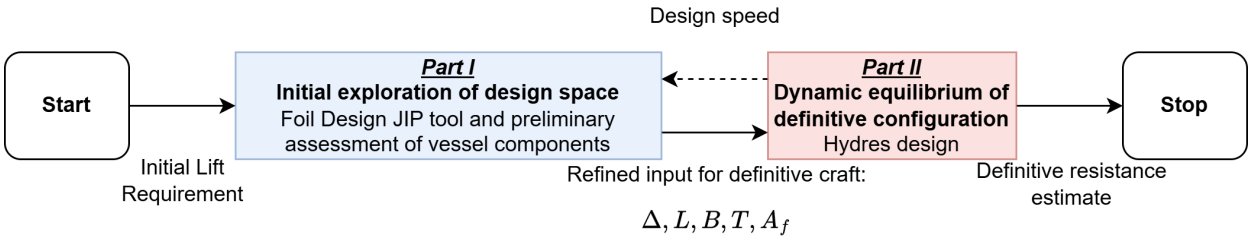

Fig. 6: Hydrofoil LAC design workflow

After Part I of the design workflow, the hydrofoil LAC is modelled in Hydres, another program developed by MARIN (van Walree, 1999). This program is able to calculate the dynamic equilibrium for a hydrofoil craft in steady condition between hull and foil bound forces, based on trim, angle of attack, and height of the vessel. Therefore, Hydres produces an estimate of resistance over the complete speed domain for the subcavitating foil region (< 50 kt). The main considerations of the program Hydres are as follows:

- Hull characteristics are based on the Series 65 model test results
- Foil characteristics are based on Prandtl's lifting line theory
- Fore-aft foil interactions are based on Prandtl's lifting line theory

- Appendage forces are obtained from empirical equations

3.2. Constraints and requirements for the hydrofoil design

Table 6 lists the parameters used for the hydrofoil designs developed within this study. The total lift is distributed by 70% to the front and 30% to the aft foil systems, as this is a generally applied lift division for this foil configuration (Yun & Bliault, 2014). Furthermore, the foils are considered constrained by the beam (B) of the vessel. The foils are modelled as carbon composite structures, with the structural properties of Godø et al. (2024).

Table 6: Main parameters of the hydrofoil design

Parameter	**Value**
Vessel trim (τ)	0° to 4°
Actuated foil angle of attack (α)	-5° to 5° (variable incidence)
Span fore foil (s)	$< B$
Lift requirement fore foil ($L_{req,fore}$)	$0.7 \cdot \Delta \cdot g$
Span aft foils (s)	$< B/2$ - 0.25 m
Lift requirement aft foils ($L_{req,aft}$)	$0.15 \cdot \Delta \cdot g$
Submergence height ($h_{submerged}$)	$\max(0.4\text{ m}, 0.85 \cdot c_{mean})$[3]
Clearance height (h_{clear})	1.25 m
Thickness to chord ratio (t/c)	0.12
Design speed (v_{design})	38 kt
Foil loading	57500 N/m^2
Equivalent sand roughness (k_s)	8 µm
Elastic modulus carbon laminate (E)	135 Gpa
Density carbon laminate (ρ_{shell})	1600 kg/m^3
Density core foam material (ρ_{core})	250 kg/m^3

3.3. Part I: Initial exploration of design space

The parametric iterative model employed for Part I is visualised in Fig. 7. The Foil Design JIP tool provides the profile and induced drag of the T-foils, including free-surface effects. A constant foil loading of 57500 N/m^2 is assumed for all foils, as this a representative foil loading for the speeds considered within the bounds of cavitation (van Walree, 1999). Assuming the maximum allowed span is optimal for a foil design, the required chord length can be derived and the necessary camber is defined. The required strut thickness is derived from Euler buckling theory following the methodology of Godø et al. (2024). Pod dimensions or required shaft diameter are derived from empirical equations (van Walree, 1998; Wartzack, 2021). The hull dimensions (L, B, T) are derived from the CB90 design, where a block coefficient (c_b) of approximately 0.61 is assumed constant for increased displacement requirements.

Additional factors need to be taken into account to retrieve the foiling resistance of a complete hydrofoil craft. These additional factors can be derived from a combination of published experimental results and empirical equations. Additional viscous resistance from surface roughness of struts and foils is estimated with the methodology of Godø et al. (2024). The additional resistance induced by the intersection between foil and strut is derived from empirical equations of Hoerner (1965). Viscous strut resistance is derived from experimental data of Abbott and Von Doenhoff (1959). Furthermore, the spray resistance from struts protruding the free-surface yields from the empirical equation of Hoerner (1965). The appendage resistance of an inclined shaft is derived with the method of Van Walree (1999), and if pods or nacelles are employed instead, their appendage resistance is derived using the drag coefficient of streamlined bodies of Hoerner (1965). Furthermore, the air resistance yields from the frontal projected area with a drag coefficient ($C_{D,air}$) of 0.5, as recommended by Faltinsen (2005).

A propulsion system can be designed based on the complete foiling top speed resistance, which is discussed in Section 3.5. The aluminium hull structural weight is based on the method of Armer (2007). The foils are assumed as solid structures, whereas the struts are defined as shells with a foam core. With the design dimensions and densities of Table 6, the foil system structural mass is derived. The outfitting weight is estimated by investigation of published data of the CB90 (Saab, 2021), which yielded an outfitting weight of 7280 kg. Lastly, the retraction system weight is derived from the estimation of Lundin and Eriksson (2021) for an electromechanical vertical retraction system. Payload and fuel mass remain inputs for the design iterations. The total displacement weight can therefore be divided as defined by Eq. (1).

$$\Delta = m_{hull} + m_{propul.} + m_{struts} + m_{foils} + m_{retract.} + m_{outfit.} + m_{payload} + m_{fuel} + m_{lub.} \tag{1}$$

[3]For optimisation the c_{mean} of the prior iteration is taken, in evaluation and results the c_{mean} of the design itself is used

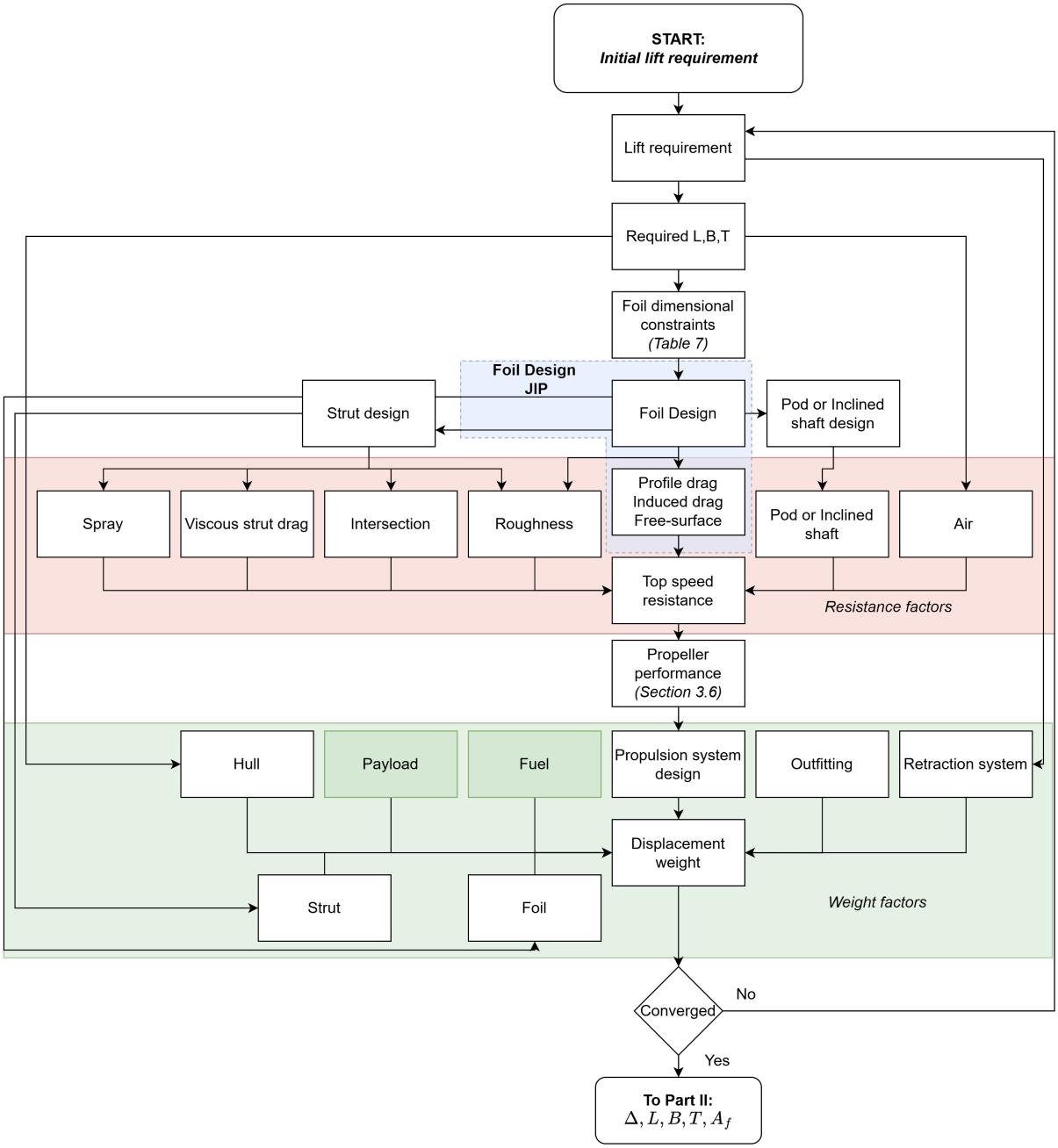

Fig. 7: Parametric model with integration of the Foil Design JIP tool for Part I

3.4. Comparison of resistance results

Fig. 8 and Table 7 show an example foil configuration for a 24.5 t design with propulsion in nacelles. This design is evaluated with the calculations of Part I (Foil Design JIP and iterative model) and Part II (Hydres). One reason for the slight variation of span and chord between the designs, is that the Foil Design JIP results require some taper of the foil, whereas the Hydres design is made rectangular without taper. The resistance results following these designs are visualised in Fig. 9. Both methods indicate that the foils will produce enough lift at the take-off speed of 25 kt. Furthermore, in both results the general trend of a high drag at take-off speed (due to a high amount of induced drag) and top speed (due to mostly viscous drag) is discerned. Overall, the drag of Part I is between 5-15% lower than the results of Hydres. This discrepancy can have several sources. Firstly, the Foil Design JIP tool has some inaccuracy due to its data-driven nature. Secondly, the interaction effects are neglected for the calculations of Part I, whereas Hydres does take this into account. The downwash of the front foil will not vary much in the spanwise direction of the aft foils however, due to the larger span of the front foil. It is therefore presumed that this error is small. Thirdly, the Foil Design JIP tool uses foil sections derived from the Eppler 817 series, whereas Hydres' foil sections are based on the NACA-66 series. The results of Part I also do not continue for speeds higher than 43 kt, as this is a limitation of the Foil Design JIP tool. After testing at multiple displacements the discrepancy remained consistent. Therefore, a margin of 10% is taken above the resistance at 43 kt of Part I, to gain a realistic estimate for the resistance at 45 kt.

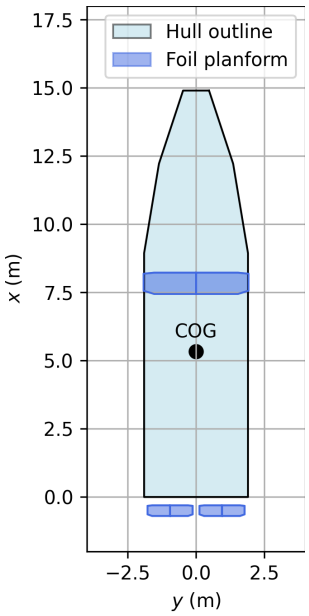

Fig. 8: Bottom side view of a 24.5 t design

Table 7: Main particulars comparison between Part I and II

Parameter	**Part I**	**Part II**	**Unit**
Displacement weight (Δ)	24500		kg
Frontal Projected Area (A_f)	11	11	m^2
c_{front}	0.77	0.76	m
c_{aft}	0.38	0.31	m
s_{front}	3.8	3.8	m
s_{aft}	1.65	1.80	m
t/c foils	0.12	0.12	-
t/c front struts	0.105	0.105	-
t/c aft struts	0.19	0.19	-

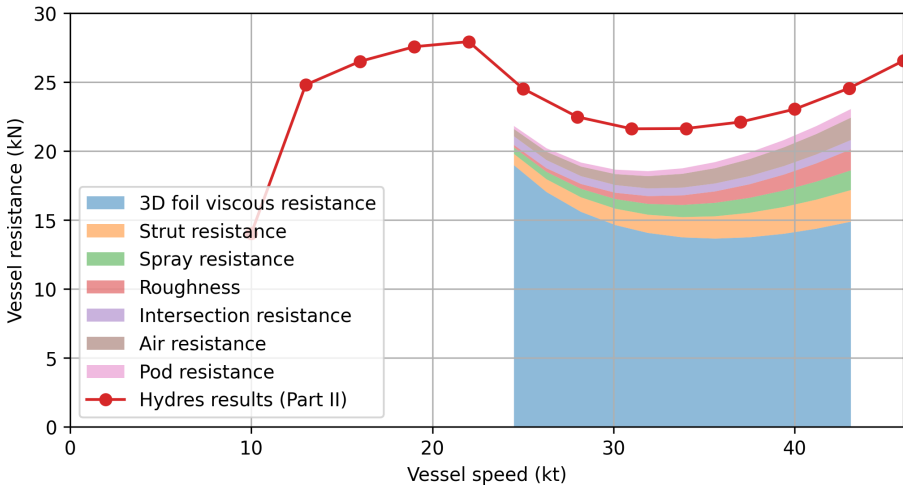

Fig. 9: Part I resistance results compared to Part II

3.5. Propulsion configurations

To assess different propulsion systems for the hydrofoil implementation, two options are considered: an inclined shaft system and an L-drive system. This also allows for a comparison between a lighter propulsion option, that has increased resistance due to an added appendage, and a heavier option that can be incorporated in a more hydrodynamically streamlined fashion. The propulsion system weight ($m_{propul.}$) is estimated by adding all weights of propulsion systems, from published supplier data.

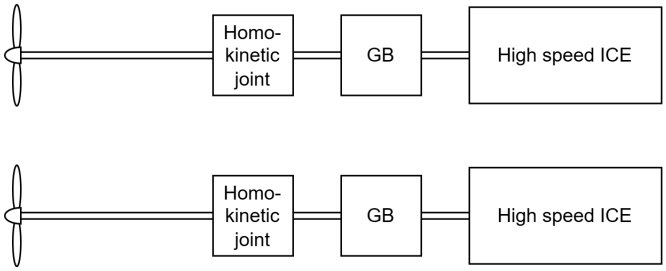

Fig. 10: Propulsion architecture of a HLAC-HK design, with a retractable inclined shaft

The inclined shaft option uses a homokinetic joint to lower the driveshaft to the required depth. This is further referred to as the Hydrofoil Littoral Assault Craft HomoKinetic (HLAC-HK) design. The configuration is visualised

in Fig. 10, with the only addition being a homokinetic joint compared to the geared drive with a gearbox (GB).

The L-drive configuration, illustrated in Fig. 11, features axial flux motors integrated at the top of the struts. This design still requires a nacelle at the bottom of the strut, incorporating a right-angle transmission. To manage transient loads in dynamic situations, such as take-off, also a 'buffer' sytem is integrated. This system may utilise supercapacitors or high-power battery modules, such as Lithium-Titanium-Oxide (LTO) batteries, to manage peak powers (Doornebos et al., 2023). The diesel-electric configuration will be referred to as the Hydrofoil Littoral Assault Craft Diesel-Electric (HLAC-DE) design.

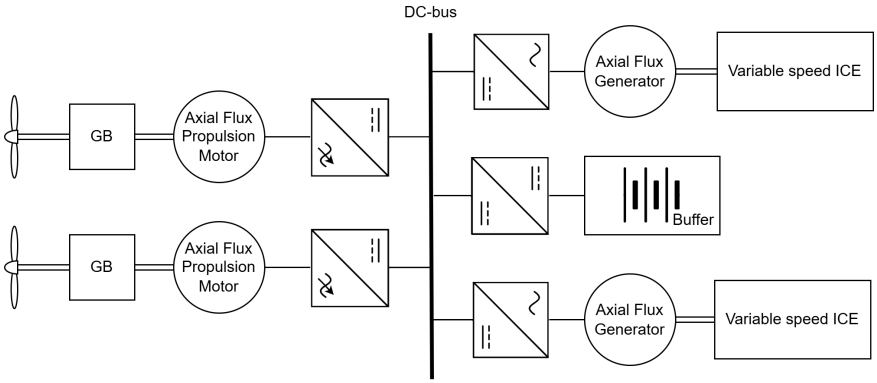

Fig. 11: Propulsion architecture of the HLAC-DE design, with the L-drive propulsion solution

3.6. *Part I: Resulting designs and weight estimates*

The calculations of Part I of the design method result in the preliminary weight estimates. The mass estimates for the HLAC-HK and HLAC-DE designs are provided in Table 9. The individual mass estimates are rounded to tens of kilograms. Furthermore, the weight estimates are compared to a prior design study of Hoerner et al. (1954), with the weight estimates of this study indicated by brackets for comparison. Although Hoerner et al. (1954) is not a recent study, it can give an indication of how the proposed designs of this thesis compare to other hydrofoil craft, and if the weight estimation calculations in this study are valid.

The mass estimates of Table 9 are generally in line with the expectations of Hoerner et al. (1954), with most weight factors not differing more than 12%. On the contrary, a large reduction can be seen in hydrofoil system weight. However, this is anticipated, as Hoerner et al. (1954) uses stainless steel for the foil structure, whereas this study employs a method based on the structural properties of carbon composites. The structural weight of the hydrofoil system is within the expectations of Godø et al. (2024), which found a weight fraction of modern carbon composite hydrofoil structures of 1-5% of the total displacement weight. Although heavier in displacement, the resistance found for the HLAC-DE configuration is lower than the HLAC-HK configuration. This is caused by the added appendage drag of an inclined shaft of the HLAC-HK configuration. For this inclined shaft, an estimated diameter of 50 mm is applied.

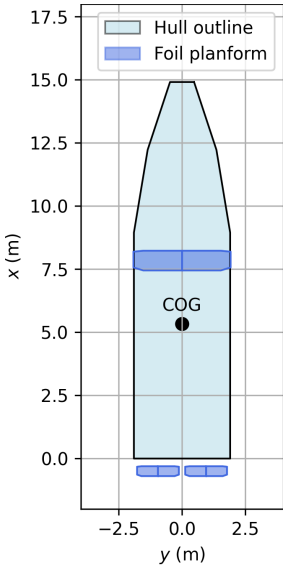

Fig. 12: HLAC-HK

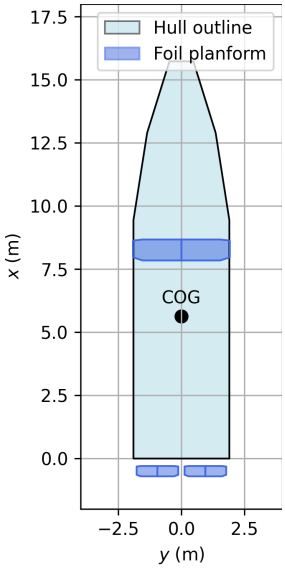

Fig. 13: HLAC-DE

Table 8: Main foil particulars of the HLAC-HK and HLAC-DE designs

Parameter	HLAC-HK	HLAC-DE	Unit
c_{front}	0.78	0.83	m
c_{aft}	0.39	0.41	m
s_{front}	3.8	3.8	m
s_{aft}	1.65	1.65	m
$camber_{front}$	5	5	%
$camber_{aft}$	4.2	4.4	%
t/c foils	0.12	0.12	-
t/c front struts	0.105	0.105	-
t/c aft struts	0.19	0.19	-

Fig 12 and 13 provide an illustration of the developed hydrofoil designs, with their main foil particulars in Table 8. From the parameters listed in Table 8 it can be gathered that the design camber is rather high, as standard foil sections are generally around 2% (Abbott & Von Doenhoff, 1959). The HLAC-HK design does not require an increase in displacement to facilitate the hydrofoil conversion. In contrast, the HLAC-DE design has a displacement increase compared to the CB90 of 6%, which increases the estimated required total length to 15.6 m. This length reaches the limits of the davits, but is still within reasonable bounds considering there is no other appendage extending the length, such as waterjet buckets.

Table 9: Weight estimates resulting of Part I of the modelling with the reference masses of Hoerner et al. (1954) in brackets

Design	**CB90**		**HLAC-HK**		**HLAC-DE**	
R @ 45 kt (kN)		38.5		30.4		27.2
η_{trm}		0.97		0.95		0.88
η_o		0.7		0.710		0.725
ε (°)		0		15		0
P_{req} (kW)		1320		1090		1030
			DWT			
Payload and fuel (kg)				***(6620)***		***(7030)***
$m_{payload}$		4500		4500		4500
m_{fuel}		1980		1980		1980
m_{lub}		80		80		80
Subtotal		6560		(-1%) 6560		(-7%) 6560
			LWT			
Hull structure and equipment (kg)				***(10790)***		***(11460)***
m_{hull}		4960		4960		5200
$m_{outfit.}$		7280		7280		7280
Subtotal		12240		(+12%) 12240		(+8%) 12480
Foil System (kg)				***(2210)***		***(2340)***
m_{foils}		-		260		300
m_{struts}		-		260		290
$m_{retract.}$		-		650		690
Subtotal		0		(-47%) 1170		(-45%) 1280
Machinery (kg)				***(4900)***		***(5210)***
m_{engine}	2x Scania DI16 077M (662 kW)	3340	2x MAN LE 426 (588 kW)	2500	2x MAN LE 446 (537 kW)	2500
m_{axconv}		-		-	2x HPIL 3 x3	1400
m_{eprop}		-		-	2x3 Emrax 348LV-LC (178 kW)	260
$m_{waterjet}$	2x Kamewa S32	1360		-		-
$m_{entrained}$		350		-		-
m_{buffer}		-		-		840
$m_{powerelec.}$		-		-		790
m_{gb}	2x Twin disc MGX 5126A	480	2x ZF 400	320		-
m_{aux}	Westerbeke (7.5 kW)	180	Westerbeke (7.5 kW)	180		-
$m_{hk,retract}$		-		1620		-
Subtotal (kg)		5710		(-6%) 4620		(+11%) 5800
LWT total (kg)		17950		18030		19480
Displacement Δ (kg)		24500		24590		26140
L (m)		14.9		14.9		15.6
B (m)		3.8		3.8		3.8
T (m)		0.86		0.86		0.86
A_f (m^2)		11		11		11

3.7. Part II: Dynamic equilibrium of definitive configuration

The resistance results using Hydres (Part II) for the HLAC-HK design are shown in Fig. 14. These results are slightly lower resistance at 45 kt than initially estimated (29.8 kN vs. 30.4 kN), but this has no impact on the propulsion system design. Thrust curves derived from a NR-series propeller are shown (Newton & Rader, 1961). As the NR-series is limited in its data to higher advance ratios, the propeller characteristics are extrapolated for the lowest vessel speeds, indicated by the dotted line. The delivered torque characteristic of a diesel engine is often assumed as a constant (Klein Woud & Stapersma, 2002). However, this assumption paints a bleak picture for the thrust produced in the

hump region. It is generally recommended to maintain a thrust margin of 20%-25% in the hump region to ensure take-off under rough sea state (Faltinsen, 2005; Johnston, 1985).

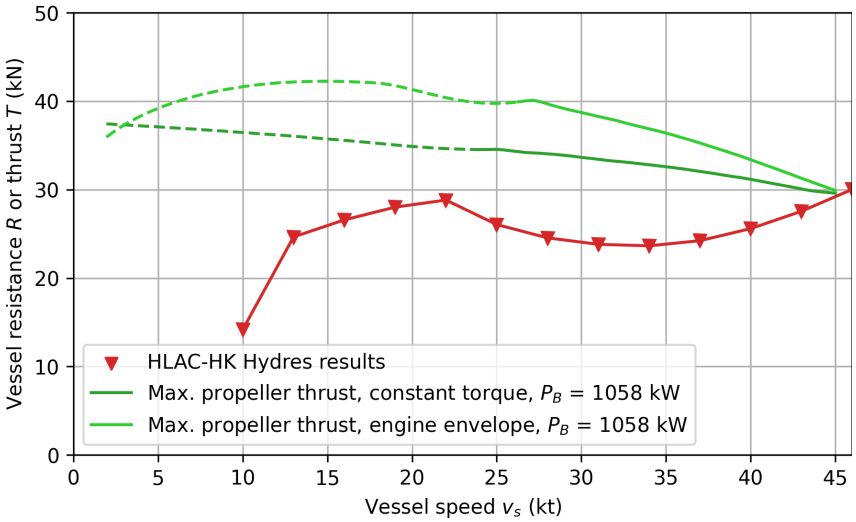

Fig. 14: Resistance and thrust curves for the HLAC-HK design

Further investigation of the modern high-speed engines in this study, indicated that relatively more torque can be produced at a moderate engine speed (Scania, 2025; Volvo Penta, 2025). This is illustrated in the engine envelope of Fig. 15, where up to 20% additional torque can be produced at lower engine speed. To visualise this significance, an additional thrust characteristic is plotted in Fig. 14 based on engine envelope, which provides ample thrust margin in the hump region.

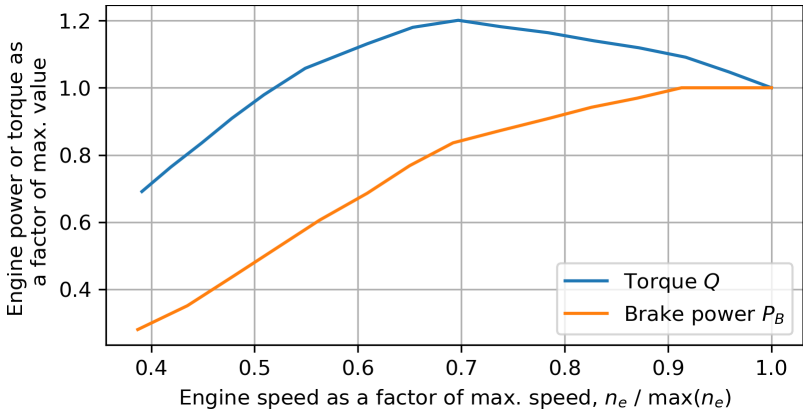

Fig. 15: Engine envelope of the Scania DI16 076M 900 HP engine, from technical specifications (Scania, 2024)

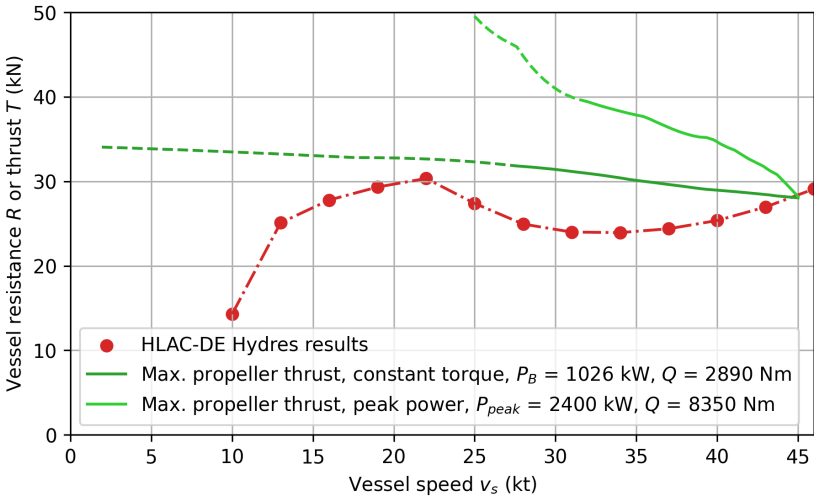

Fig. 16: Resistance and thrust curves for the HLAC-DE design

Fig. 16 presents the thrust and resistance curve of the HLAC-DE design. While the resistance at 45 kt is slightly higher than initially estimated (28.4 vs. 27.2 kN), this does not impact the weight estimation. Assuming constant torque will result in critically low thrust in the hump region again. However, the axial flux propulsion motors of this design can provide peak torque and power for brief periods of time. This can be more than two times the nominal torque and power (Beyond Motors, 2025; Emrax, 2025; Evolito, 2025). The duration of this peak condition is limited, typically between 10 to 60 seconds. Research on boosting methods indicates that, with enough thrust margin, 10 seconds of peak thrust suffices for take-off (Minerva & Montero, 2021). With the proposed installed generator power (See Table 9), enough power is generated to advance through the hump region up to 54 kN, which vastly exceeds the requirement. Thus, no additional power delivery is required.

3.8. Resistance and range comparison

Fig. 17 compares the different designs on their calm water resistance development. Furthermore, a reference resistance of a planing benchmark vessel is provided. For the lower vessel speed region, an estimation by the Delft Systematic Deadrise Series is provided (Keuning & Hillege, 2017), but this series is limited in its speed range and therefore also the estimation method of Savitsky (1964) is shown for the highest velocities.

Both hydrofoil designs have a higher resistance curve than was previously seen in Fig. 9. For the HLAC-HK, this is caused by the added appendage drag of an inclined shaft, whereas the HLAC-DE design increases its resistance due to a heavier propulsion system. These different types of drag increase also result in a differing resistance characteristic: the HLAC-DE resistance has a higher hump region resistance, whereas the HLAC-HK has a higher top speed resistance. For both hydrofoil designs, there is a region from 27 kt to 40 kt where the resistance is substantially lower than the planing benchmark. The planing CB90 derived design has a resistance around 38 kN, whereas the hydrofoil designs have a resistance around 25 kN. This is a drag reduction of approximately 35%.

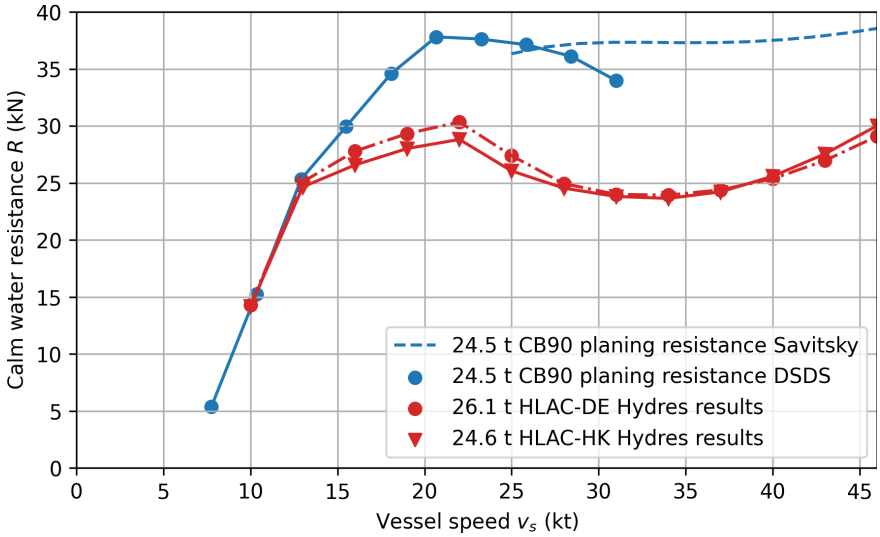

Fig. 17: Resistance development of different designs

Based on the derived resistance, the Overall Propulsive Coefficient (OPC), and the Specific Fuel Consumption (sfc), the range of each vessel is evaluated. The OPC is the product of transmission and propulsive efficiency, as defined by Eq. (2). The conventional range equation is defined by Eq. (3), where L and D denote the total lift (weight) and drag of the vessel at a given speed (McKesson, 2014). However, this formulation assumes constant displacement, meaning that resistance and power remain unchanged even as fuel is consumed during sailing. This assumption can misrepresent the range of long-range advanced marine vehicles. The Breguet formula (Eq. (4)) introduces a logarithmic term, to reflect the vessel's weight reduction as fuel is burned. Instead of assuming constant displacement, this equation assumes constant L/D (McKesson, 2014).

$$OPC = \eta_{trm} \cdot \eta_D \tag{2}$$

$$\frac{m_{fuel}}{\Delta} \cdot 198 \cdot 10^3 \cdot OPC \cdot \frac{L}{D} \cdot \frac{1}{sfc} \tag{3}$$

$$-\ln\left(1 - \frac{m_{fuel}}{\Delta}\right) \cdot 198 \cdot 10^3 \cdot OPC \cdot \frac{L}{D} \cdot \frac{1}{sfc} \tag{4}$$

To analyse the relation between speed and energy consumption, also the transport efficiency can be evaluated (Trancossi, 2016). First defined by Gabrielli and von Karman (1950), the analysis introduces a physical parameter, named specific resistance (ε) of the vehicle. It represents the ratio between the required power divided by the total

vehicle weight times its speed. This can also be defined for a payload weight, as in Eq. (5). The inverse of specific resistance represents the transport efficiency.

$$\varepsilon_{payload} = \frac{P}{m_{payload} \cdot g \cdot v_s} \tag{5}$$

Table 10 lists performance characteristics of the designs introduced in this chapter. it is assumed that the sfc is a constant for each design. Both hydrofoil designs can increase the range of the vessel with around 50% in calm water. Additionally, the payload transport efficiency is increased with aproximately 45% for cruising speed and 30% for top speed. Both hydrofoil designs show similar performance characteristics. However, the HLAC-DE design has a higher L/D characteristic. It is therefore expected that, if weight saving measures are applied, the gains in resistance reduction will be larger for the HLAC-DE design. The HLAC-HK will keep approximately the same appendage drag due to the inclined shafts, whereas the HLAC-DE design's nacelle drag will remain relatively small.

Table 10: Performance characteristics of hydrofoil designs compared to the planing benchmark design

Design	**CB90**	**HLAC-HK**	**HLAC-DE**
Displacement weight Δ (t)	24.5	24.6	26.1
OPC @ 45 kt (-)	0.68	0.66	0.64
OPC @ 30 kt (-)	0.68	0.64	0.62
sfc (g/kWh)	205	205	205
L (kN)	240	241	256
D @ 30 kt (kN)	37.5	24.5	24.5
L/D @ 30 kt (-)	6.4	9.8	10.4
P_{cruise} @ 30 kt (kW)	850	590	610
P_{req} @ 45 kt (kW)	1320	1090	1030
Constant displacement range @ 30 kt (10% fuel reserve) (nm)	295	440	430
Breguet range @ 30 kt (10% fuel reserve) (nm)	310	460	440
$1/\varepsilon_{payload}$ @ 30 kt (-)	0.80	1.15	1.12
$1/\varepsilon_{payload}$ @ 45 kt (-)	0.77	0.94	0.99

4. Weight saving measures

The developed design method can be utilised to analyse the effect of weight saving measures. Table 11 presents several weight saving measures identified for a future LAC design. The relative weight saving of applying a Carbon Fibre Reinforced Hull (CFRP) structure is identified as the measure with the largest relative weight saving, based on several design studies (Gurit, 2015; Oh et al., 2018; Olofsson et al., 2008; Stenius et al., 2011). The other weight saving measures reduce some capabilities vessel to identify the gains that can be achieved in other aspects, such as reduced resistance or system requirements.

Table 11: Weight saving measures identified for a hydrofoil LAC, based on the HLAC-DE design

Measure	**A. CFRP composite hull**	**B. Constant range (300 nm)**	**C. Reduced outfitting**	**D. Reduced payload**
Original weight (kg)	5200	1980	7280	4500
Original weight fraction	20%	8%	30%	18%
Weight saving within weight fraction	50%	Design dependent	30%	36%

The resulting resistance curves of applying weight saving measures are plotted in Fig. 18. Each design is given an indicator which stands for the measures taken in the design, preceded by "M" for measure. This implies that design M.ABCD has all measures taken into account. The hump resistance decreases proportionally to the decrease in foiling resistance, where the foiling top speed resistance has approximately the same magnitude as the maximum hump resistance. Investigation of the drag calculations reveals that the L/D increases as the weight of the vessels is reduced. This implies that the resistance does not reduce linearly for a lower displacement, but has an exponential factor. Therefore, the resistance for different displacements at 30 kt can be illustrated as in Fig. 19a, with an exponential fit. Furthermore, this can be reasoned backwards to the direct weight saving that is realised. Fig. 19b shows how the direct weight saving (excluding fuel, propulsion, and foil system weight) affects the resistance reduction. This follows an inverse exponential relation, meaning that the largest reductions in resistance can be found for the lowest reductions

in weight. As an example, 5% in direct weight reduction already accounts for a 12% reduction in resistance. However, for the highest weight reduction of 30%, the resistance is reduced with 50%.

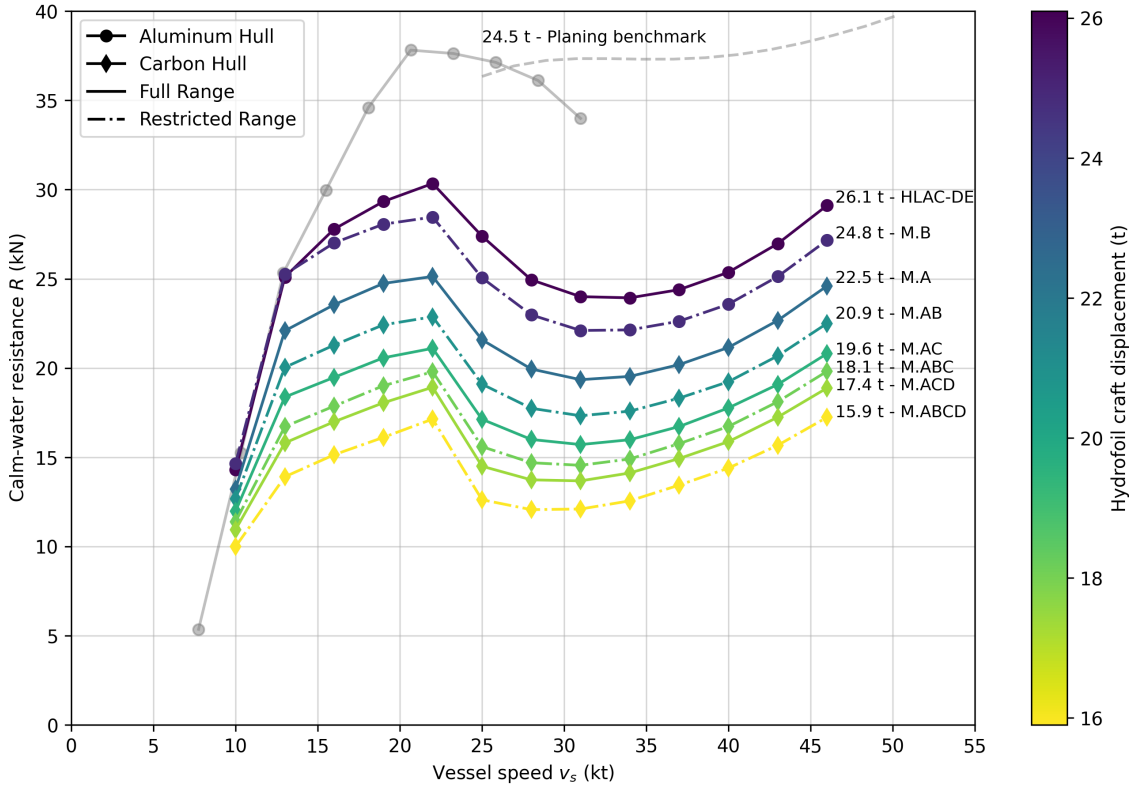

Fig. 18: Several HLAC-DE designs with weight saving measures

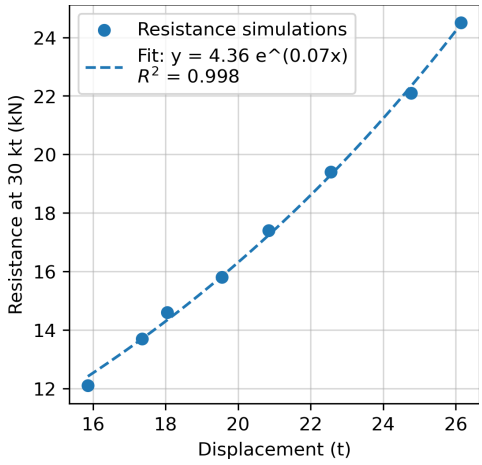

(a) Resistance for different displacements

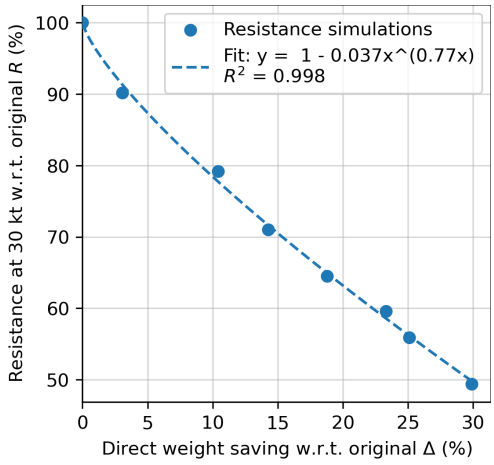

(b) Direct weight saving effect for the HLAC-DE design

Fig. 19: Impact of weight saving measures

5. Seakeeping performance

For seakeeping assessment of a planing hull and hydrofoil design the program Panship is utilised (van Walree, 2002). This is a time domain panel method based on the transient free surface Green function to incorporate wave-making effects (van Walree, 2015). The free-surface conditions are linearised around the mean free surface, enabling the hydrodynamic problem to be solved using panels only on the ship's surface.

PanShip consists of two versions: a semi-linear (PanShip) and a semi-nonlinear version (PanShipNL). PanShip uses the mean wetted body surface at speed for radiation and diffraction forces, while using the instantaneous wetted body surface for the undisturbed wave forces. This approach is numerically efficient as the most computationally demanding tasks are performed only once. In contrast, PanShipNL uses the instantaneous wetted surface for all hydrodynamic forces, providing greater accuracy. The final simulation is conducted as a run of 15000 time steps of 0.030 s. This

results in a total simulation time of 450 s. The planing hull uses the PanShipNL method, whereas the hydrofoil design uses the PanShip version. As the wetted surface-area of the hydrofoil design does not change significantly in waves, the semi-linear PanShip method is considered as an accurate simulation.

Fig. 20a visualises the planing benchmark hull. Although inspired by the CB90, this design is an independent creation, and no direct conclusions should be drawn about the CB90 itself. The design features a deadrise angle (β) of 20° and a hard chine. Fig. 20a also shows the dynamic pressure (C_{pu}) that can occur in waves for this hull in the prescribed sea state of Table 12. The substantial dynamic pressure at the bow hatch indicates that this can be a source for slamming forces. In a test run at full displacement (Δ = 24.5 t), unrealistically high forces were excited on the vessel due to bow diving. Because of this, the displacement is reduced to 21.0 t, which allows the vessel to remain mostly in planing mode in this dynamic condition.

Fig. 20b visualises how the hydrofoil design is modelled in PanShip. The geometry is based on the Hydres output of the example hydrofoil design of Section 3.4. This is the design for a 24.5 t hydrofoil craft, without additional considerations for added weight of the propulsion or hydrofoil system. Additionally, no nacelles or other appendages are modelled. The motion control of the vessel is realised by a flap motion control system. It utilises a PID-controller with gains based on experience of van Walree (2025). The vessel remains in platforming mode for this condition, meaning that the vessel sails above the waves, as opposed to riding along the waves in a contouring mode (Faltinsen, 2005). Contouring is generally employed when the wave encounter frequency is low, whereas a platforming mode is applied for a high wave encounter frequency (Faltinsen, 2005).

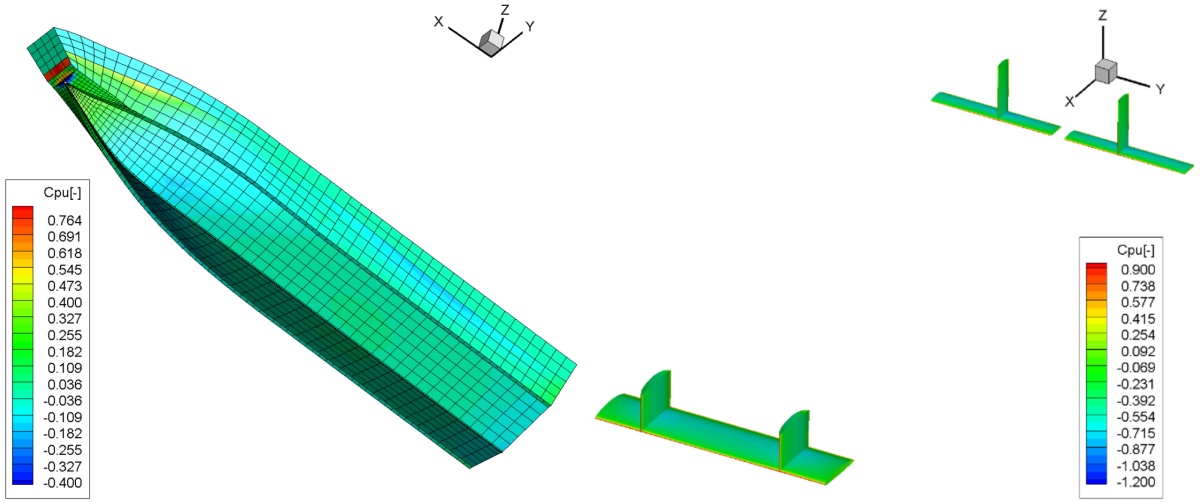

(a) Planing hull (PanShipNL)

(b) Hydrofoil design (PanShip)

Fig. 20: Vessels modelled in PanShip and PanShipNL

The simulation in PanShip is conducted with expert support from the software's developer, Frans van Walree, who modelled the two cases within PanShip. This ensures that the study provides accurate results within its time constraints. The input of the planing hull and hydrofoil design, wave conditions, and subsequent analysis are provided by the author.

The modelled irregular wave condition for the simulation follows the Joint North Sea Wave Project (JONSWAP), with the parameters listed in Table 12. This is the most probable condition for a significant wave height of 1.25 m at the Gemini wind park, which is located around 45 nm from the Dutch coastline (Brans, 2021).

Table 12: Sea state considered for seakeeping analysis

	Significant wave height	**Peak period**	**Mean centroid wave period**	**Mean zero-crossing wave period**	**Peakedness factor**	**Wave direction**	**Vessel speed**
Symbol	$H_{1/3}$	T_p	T_1	T_2	γ	μ	v_s
Value	1.25 m	5.75 s	4.79 s	4.43 s	3.3	180°	35 kt

5.1. Peak vertical accelerations

Keuning (1994) identified the peak value of vertical accelerations as the limiting factor of high-speed craft operations, which cannot be drawn out of standard deviations directly. As PanShip is a time-domain method however, these peak vertical accelerations can be derived for both vessels. The probability of acceleration exceedance can be plotted in a Rayleigh plot, such as shown in Fig. 21. The vertical accelerations can reach peak values of approximately 10 g

(g = 9.81 m/s^2). These accelerations can be sustained by personnel for a short period of time if shock-mitigating seats are used, as measurements on other high-speed military craft have recorded accelerations up to 15 g (Margés, 2018). However, it is unreasonable to expect that this can be sustained by personnel for the extended transit duration of future landings, which will take more than one hour. Around 15% of the peak vertical accelerations at the Centre of Gravity (CoG) are higher than 1.25 g (12.3 m/s^2). Based on the consideration of Keuning (1994) that professional crews will reduce their speed when peak accelerations of 1.25 g are experienced, the vertical acceleration at this speed is considered unsustainable (Deyzen, 2013).

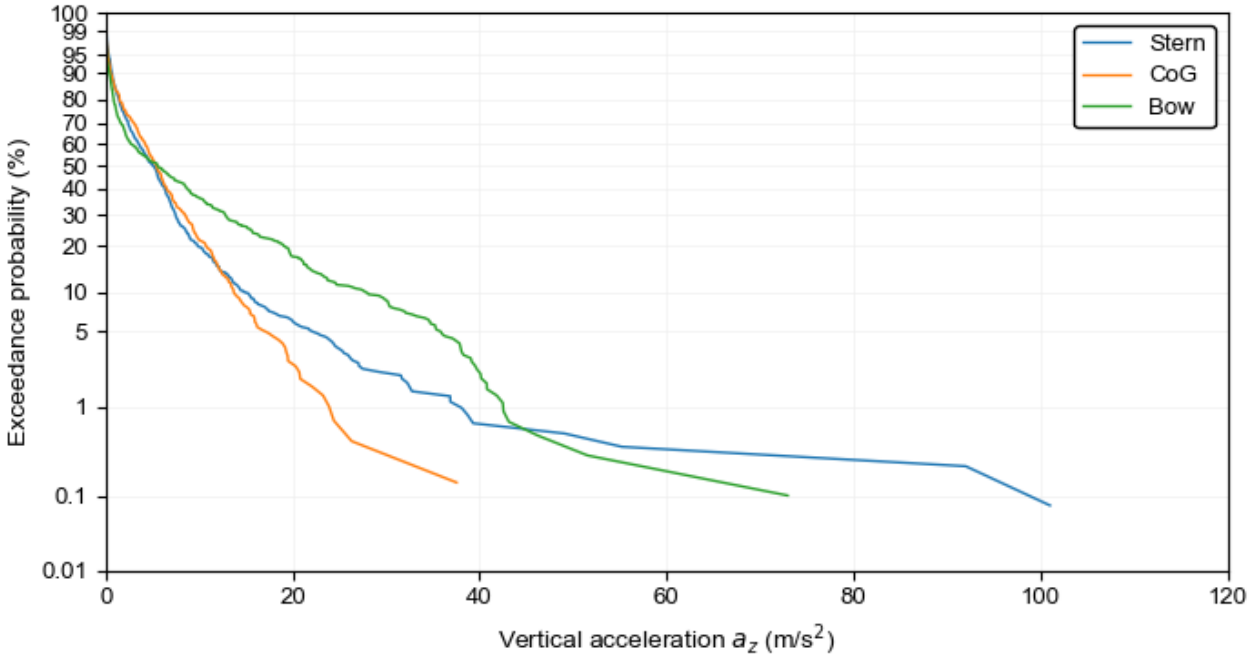

Fig. 21: Acceleration distribution of the planing hull in a Rayleigh plot

Fig. 22 shows the vertical accelerations experienced by the foiling craft design. It is important to note the difference in scale compared to note the scale difference with Fig. 21, as far lower accelerations are experienced. Furthermore, in contrast to the planing hull, an almost Rayleigh distributed relation is found between exceedance probability and vertical acceleration. This indicates that an almost linear motion is experienced by the hydrofoil craft with respect to the incoming waves. Moreover, the 1/1000th vertical accelerations are reduced with approximately 90%, from 38 m/s^2 to 2.8 m/s^2, at the CoG.

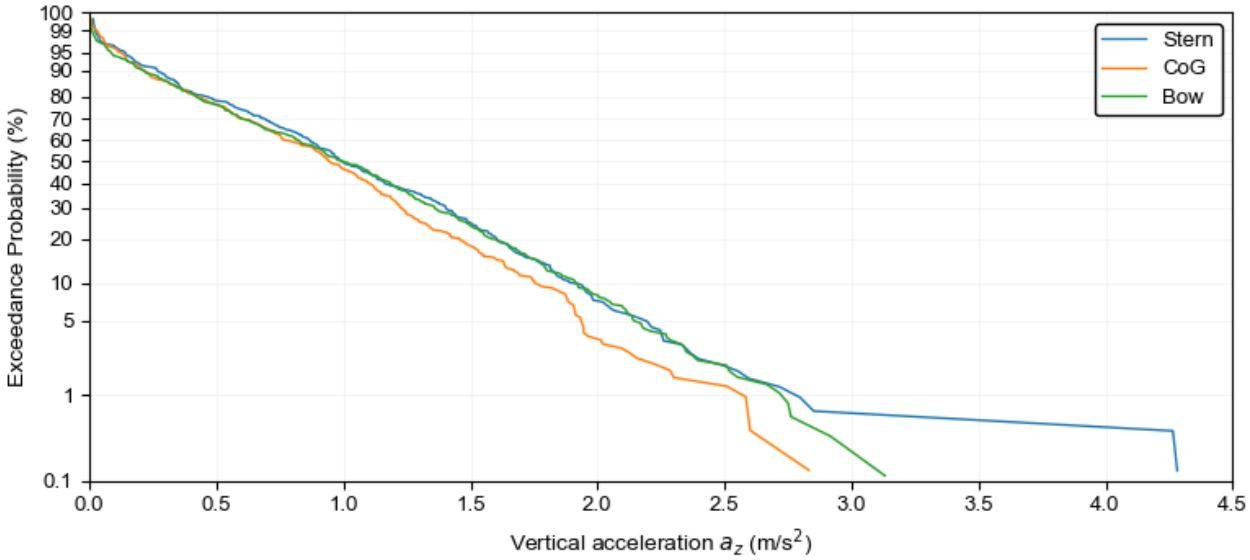

Fig. 22: Acceleration distribution of the hydrofoil craft in a Rayleigh plot

5.2. *Required strut length*

To analyse if the designed strut length of the hydrofoil design is sufficient, the relative wave height of the vessel is investigated. The relative wave height is a variable to measure the possibility of foil-water surface penetration, and slamming (Faltinsen, 2005). Both situations will cause stability problems for the foiling craft. The time trace of Fig. 23 illustrates that the designed foil submergence of the front foil (1 m) is sufficient, however, the aft foil still reaches negative relative wave heights. With an increase of the aft foil submergence from 0.8 m to 1 m, foil submergence can be guaranteed.

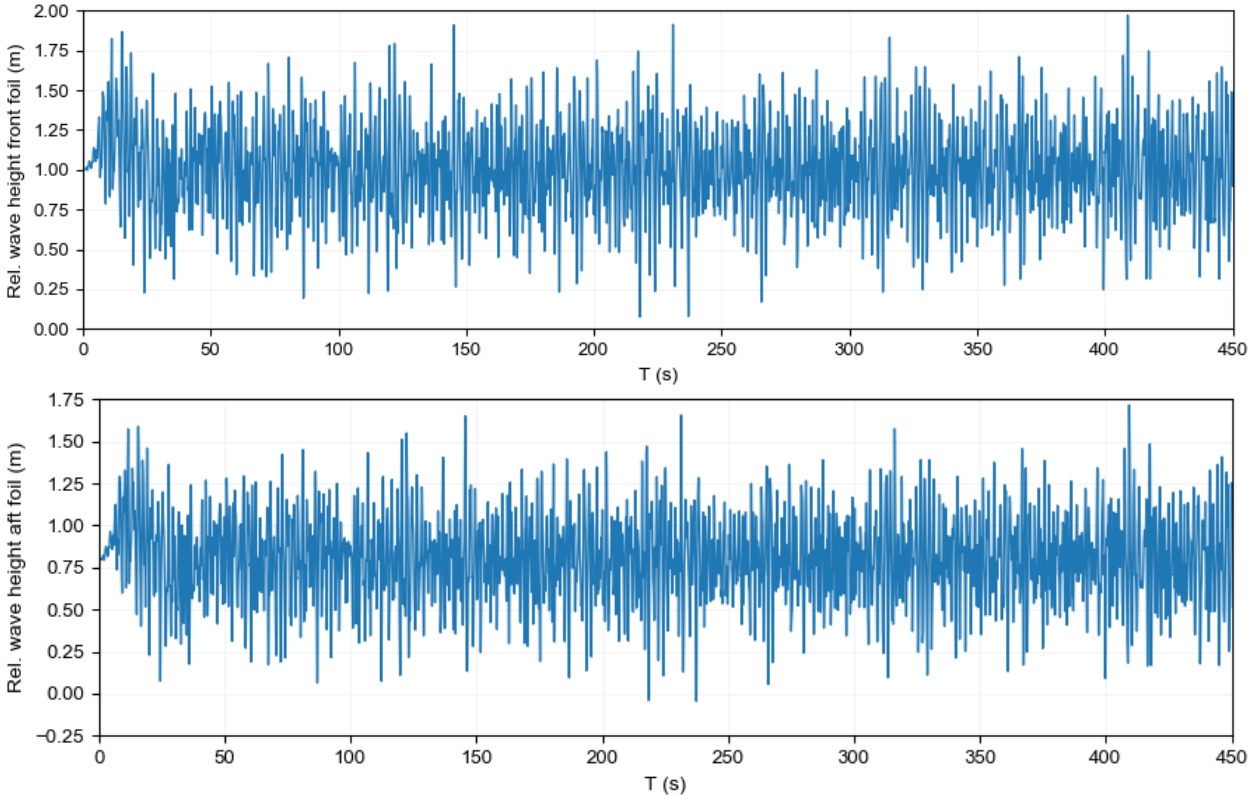

Fig. 23: Relative wave height with respect to front and aft foils

Fig. 24 visualises the relative wave height with respect to the Front PerPendicular (FPP) of the hydrofoil vessel. From the time trace, it can be derived that the waves oscillate around the mean value of 1.25 m, which is the design clearance height (h_{clear}). The relative wave height should remain below 0 to prevent waves hitting the hull bottom. If the relative wave height would become higher than 0, it could result in a slamming force that destabilises the vessel. However, the waves do not reach the hull bottom and a margin of 0.25 m is left. Due to having this margin, it is concluded that this hull clearance is over-dimensioned.

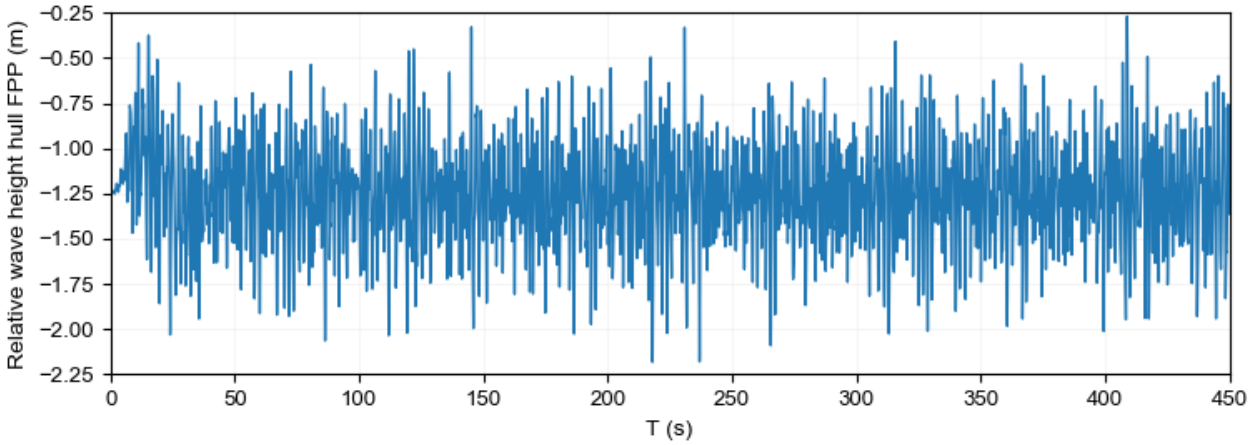

Fig. 24: Relative wave height with respect to the Front Perpendicular (FPP) on the baseline

Based on the relative wave motions of the hydrofoil craft, it can be derived that struts extending the hull with two

meter (front and aft) guarantees foil submergence and no wave contact with the hull in this sea state. This would require one meter of mean submergence depth, and another meter for mean hull clearance. The length that the strut extends from the hull can then be defined as in Eq (6), where $h_{ext,strut}$, T_{foil}, and T denotes strut extension length, draft with foils extended, and hull draft, respectively. The extension height is also referred to as the effective height (van Oossanen, 1983).

$$h_{ext,strut} = T_{foil} - T = h_{clear} + h_{submerged} \tag{6}$$

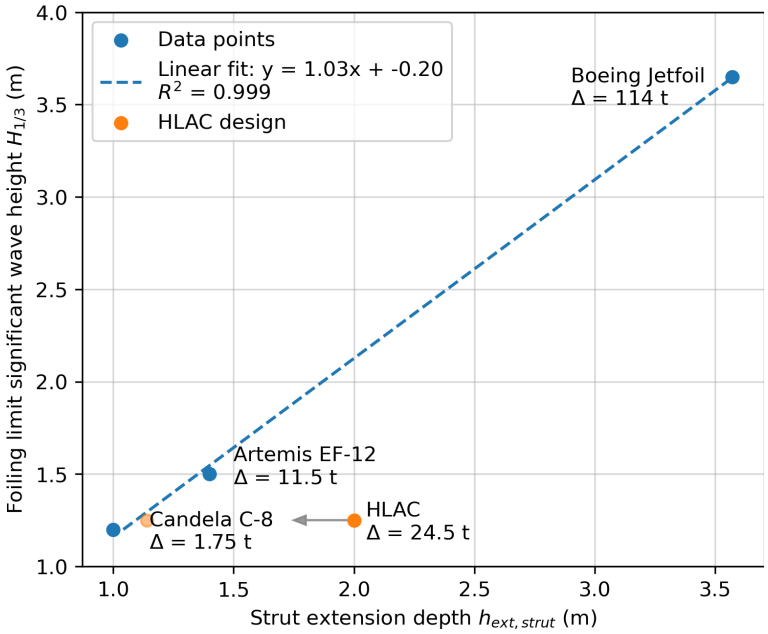

Fig. 25: Limiting significant wave height for several monohull submerged hydrofoil designs (Candela, 2024b; Cauwenberghe, 2025; Yun & Bliault, 2014)

However, investigation of the claims of hydrofoil craft manufacturers indicates that a limited amount of wave contact with the hull can be permitted. The strut extension length of several hydrofoil craft can be plotted as in Fig. 25. Although the amount of data points is limited, a linear relation can be derived between strut length and the limiting sea state. As this is based on significant wave height, defined as the mean wave height (trough to crest) of the highest third of the waves ($H_{1/3}$), higher wave heights will also be encountered by these vessels (Journee et al., 2015). Although the amount of data points is limited, a linear relation can be derived between strut length and the limiting sea state. It should be noted that sea state is not only dependent on the significant wave height, as seen in Table 12. Nevertheless, it provides an indication of how hydrofoil craft manufacturers relate their operability limitations to strut design. Generally, the limiting significant wave height is slightly higher than the strut extension depth. While a longer strut length improves operability, it also makes stabilization more challenging and demands greater structural strength. Fig. 25 therefore suggests that the strut length can be reduced to attain similar seakeeping performance.

6. Conclusion

This study explored the potential of integrating hydrofoil systems into a future LAC design. To investigate this potential, a design method is developed and two types of propulsion systems are evaluated: an inclined shaft system (HLAC-HK) and a diesel-electric L-drive system (HLAC-DE). Both propulsion systems have the capacity to transition through the hump region without additional power requirements. However, both configurations have drawbacks that result in a higher resistance. The HLAC-HK design has additional appendage drag due to the inclined shaft, and the HLAC-DE design has increased resistance due to a heavier propulsion system compared to the HLAC-HK design. Nonetheless, the resistance reduction compared to the planing benchmark vessel, with the same payload carrying capacity, can be up to 35%. This leads to the first MoE of the implementation of hydrofoils, as they can realise a range increase of approximately 50% at 30 kt. Conversely, maintaining the HLAC-DE's range equivalent to the planing benchmark vessel can realise a similar displacement. In addition, the effect of weight saving measures on the hydrofoil craft design is evaluated. The analysis reveals an inversely exponential relationship between weight reduction and resistance, highlighting the value of weight saving efforts.

To assess the seakeeping performance of a hydrofoil craft compared to a planing vessel, time-domain simulation method PanShip is applied. The analysis considers the worst condition in sea state 3 ($H_{1/3}$ = 1.25 m, T_p = 5.75 s) 45 nm of the Netherlands' coast. Results show that a planing hull cannot sustain 35 kt in these conditions due to excessive

vertical accelerations, reaching peak accelerations up to 10 g. In contrast, the hydrofoil design diminishes the induced wave motions and accelerations significantly. Peak vertical accelerations are reduced by 90% at the CoG.

Table 13 lists the results of this study by providing a comparison between the planing benchmark vessel (based on the CB90) and the proposed HLAC designs. Although limited in the amount of performance indicators, it provides an indication of the potential of submerged hydrofoil systems through the use of MoEs. While the addition of a retractable hydrofoil system introduces considerable design complexity, the results demonstrate the potential of submerged hydrofoil systems to enhance operational performance of a future LAC design.

Table 13: Design drivers and Measures of Effectiveness (MoE) of a future LAC

Design Driver	**Criteria to improve compared to base design (MoE)**	**Current requirement**	**Base value planing hull**	**HLAC foiling craft**
Range	Nautical miles in high speed (30 kt) calm water	200 nm	300 nm	$\approx$ 450 nm (+50%)
Speed	Maximum sustained speed in sea state 3	25 kt	$<$ 35 kt	$>$ 35 kt (+)
Safety	A1/10 positive vertical accelerations in sea state 3 at 35 kt on CoG	35 m/s^2	20 - 30 m/s^2	2 - 2.3 m/s^2 (-90%)

7. Recommendations

The following main recommendations are proposed from this study:

- **Weight saving measures:** The results of this study substantiate that the gains of weight saving measure can have a large effect on the requirements posed on the propulsion system and the performance of the design. Therefore, the further investigation of applying composite materials to the hull structure is of interest. Furthermore, reducing outfitting, fuel, or payload weight where possible can produce more efficient hydrofoil designs. Thorough investigation of these weight factors on current craft can make clear how much weight saving can be realised.
- **Edge cases for operability:** Submerged hydrofoil craft have a unique dynamic stability characteristic, which makes rise to edge cases which should also be analysed before safe operation can be commenced. Scenarios such as nose-diving due to foil ventilation or foil broaching severely affect the safe operation of these craft. Testing with USVs can offer a solution to test control strategies at high speeds at (near) full scale, before implementing these for vessels intended for passenger transfer. Furthermore, a worst-case scenario simulation with foil broaching can provide insight in additional safety measures that need to be taken. This can also provide insight in how CoG placement can affect the nose-diving behaviour of the craft.
- **Seakeeping assessment with hull effects:** A comparison of similar monohull hydrofoil craft makes clear that a limited amount of hull-wave interaction is permitted for monohull hydrofoil designs without stability issues. It is therefore of interest to investigate the amount of hull-wave submergence is possible, before the hydrofoil design becomes unstable. The result of this assessment can provide better requirements for the strut length.

Acknowledgements

The PanShip simulations provided in this paper are conducted with expert support from the program's developer, Frans van Walree, who modelled the two cases within PanShip. The input of the planing hull and hydrofoil design, wave conditions, and subsequent analysis are provided by the lead author. The authors would like to thank the Maritime Research Institute Netherlands (MARIN) for providing this support, which was instrumental to the completion of this research.

This work was carried out as part of the master's thesis of the author R.M. Zwinkels (2025), in collaboration with De Haas Shipyards and MARIN. Supervision during the project was provided by J.L Gelling, R. Kalisvaart, L.F. Minerva, and A.A. Kana. The work should therefore be viewed as independent research conducted for assessment by Delft University of Technology, and not as part of any tender procedure.

Declaration of AI-assisted technologies in the writing process

During the preparation of this work, the lead author used the AI-based language model ChatGPT by OpenAI, in order to improve the spelling, language, and grammar of this paper. After using these services, the author reviewed and edited the content as needed and takes full responsibility for the content of the publication.

Nomenclature

Abbreviation	Definition
A1/10	Mean value of 10% highest peaks
AC	Alternating Current
AMV	Advanced Marine Vehicles
BAR	Blade-Area Ratio
CB90	Combat Boat 90
CoG	Centre of Gravity
CZSK	Commandant Zeestrijdkrachten (Commander of the naval forces)
DC	Direct Current
DSDS	Delft Systematic Deadrise Series
DWT	Deadweight
FPP	Front PerPendicular
FLitOC	Future Littoral Operating Concept
HF REQ	Hydrofoil system requirement
HLAC	Hydrofoil Littoral Assault Craft
HLAC-DE	Hydrofoil Littoral Assault Craft Diesel-Electric design
HLAC-HK	Hydrofoil Littoral Assault Craft HomoKinetic design
ICE	Internal Combustion Engine
JSS	Joint logistic Support Ship
LAC	Littoral Assault Craft
LCM	Littoral Craft Mobility
LCVP	Landing Craft Vehicle Personnel
LCU	Landing Craft Utility
LPD	Landing Platform Dock
LWT	Lightweight
MARIN	MAritime Research Institute Netherlands
MoE	Measure of Effectiveness
NLMOD	Netherlands Ministry of Defence
NR	Newton-Rader
RNLN	Royal Netherlands Navy
RNMC	Royal Netherlands Marine Corps

Symbol	Definition	Unit
-	Range	nm (1852 m)
A_f	Frontal projected area	m^2
a_z	Heave acceleration	m s^{-2}
B	Vessel beam	m
C_{pu}	Dynamic pressure coefficient	-
c	Foil chord length	m
c_b	Hull block coefficient	-
$camber$	Camber	-
c_{aft}	Aft foil chord length	m
c_{front}	Front foil chord length	m
c_{mean}	Foil mean chord length	m
D_{max}	Maximum propeller diameter	m
E	Elastic modulus	GPa
$H_{1/3}$	Significant wave height	m
h	Height	m
h_{clear}	Clearance height	m
$h_{ext,strut}$	Strut extension length	m
$h_{submerged}$	Submergence height	m
g	Gravitational acceleration	9.81 m s^{-2}
J	Advance ratio	-
K_T	Thrust coefficient	-
$K_{T,ship,0}$	Vessel design thrust coefficient	-
K_Q	Torque coefficient	-

Symbol	Definition	Unit
k_s	Equivalent sand roughness	µm
L	Lift	N
L	Vessel length	m
L_{oa}	Vessel length over all	m
$L_{req,fore}$	Fore foil lift requirement	N
$L_{req,aft}$	Aft foil lift requirement	N
R	Resistance	N
s	Span length	m
s_{aft}	Aft foil span length	m
s_{front}	Front foil span length	m
sfc	Specific fuel consumption	g/kWh
T	Vessel draught	m
T_p	Peak period	s
t	Foil thickness	m
m	Mass	kg
m_{aux}	Auxilliary genset mass	kg
m_{axconv}	Axial flux motor conversion mass	kg
m_{buffer}	Buffer system mass	kg
$m_{entrained}$	Waterjet entrained water mass	kg
m_{engine}	Internal combustion engine mass	kg
m_{eprop}	Electrical propulsion motor mass	kg
m_{foils}	Foil structural mass	kg
m_{fuel}	Fuel mass	kg
m_{genset}	Generator set mass	kg
m_{gb}	Gearbox mass	kg
$m_{hk,retract}$	Homokinetic retraction system mass	kg
m_{hull}	Structural hull mass	kg
$m_{outfit.}$	Outfitting mass	kg
$m_{powerelec.}$	Power electronics mass	kg
$m_{waterjet}$	Waterjet mass	kg
m_{lub}	Lubrication oil mass	kg
$m_{payload}$	Payload mass	kg
$m_{propul.}$	Propulsion system mass	kg
$m_{retract.}$	Foil retraction system mass	kg
m_{struts}	Strut structural mass	kg
N	Normal force	N
n	Quantity	-
n_e	Rotational engine speed	s^{-1} (Hz)
n_{opt}	Optimal propeller speed	s^{-1} (Hz)
OPC	Overall propulsive coefficient	-
v_a	Advance velocity	m s^{-1}
v_s	Vessel speed	kt (1852/3600 m s^{-1})
v_{design}	Foil design speed	kt (1852/3600 m s^{-1})
P	Power	W
P_{cruise}	Cruise power	W
P_B	Brake power	W
P_{req}	Required installed power	W
α	Angle of attack	rad
β	Deadrise angle	rad
Δ	Displacement mass	kg
δ	Flap angle	rad
ε	Inclination angle	rad
$\varepsilon_{payload}$	Payload specific resistance	-
τ	Trim	rad
η_e	Engine efficiency	-
η_D	Propulsive efficiency	-
η_o	Open water efficiency	-
η_{trm}	Transmission efficiency	-

Symbol	Definition	Unit
ρ_{shell}	Density carbon laminate	kg m^{-3}
ρ_{core}	Density foam core material	kg m^{-3}
ρ_{sw}	Sea water density	kg m^{-3}
σ_0	Propeller cavitation number	-

References

ABB. (2022). Product data sheet hes880 traction inverter motor and generator application [retrieved 14-02-2025]. https://search.abb.com/library/Download.aspx?DocumentID=9AKK108467A0006&LanguageCode=en&DocumentPartId=&Action=Launch

ABB. (2023, July). Low voltage water-cooled motors [catalog]. https://search.abb.com/library/Download.aspx?DocumentID=9AKK104379&LanguageCode=en&DocumentPartId=&Action=Launch

Abbott, I., & Von Doenhoff, A. (1959). *Theory of wing sections, including a summary of airfoil data*. Dover Publications. https://books.google.nl/books?id=DPZYUGNyuboC

Ardon, A. (2008). Swedish combat boat 90 (cb 90) in the port of gothenburg stridsbåt 90 [licensed under the Creative Commons Attribution-Share Alike 2.0 Generic license.]. https://commons.wikimedia.org/wiki/File:Stridsb%C3%A5t_90.jpg

Armer, S. (2007). Estimated hull weight. https://www.boatdesign.net/threads/hull-aluminium-weight.15770/

Artemis. (2024). *Ef-24 passenger ferry* [retrieved 11-6-2024]. https://www.artemistechnologies.co.uk/ef-24-passenger-ferry/

Beyond Motors. (2025). E-motors [retrieved 28-1-2025]. https://www.beyondmotors.io/e-motors

Bieker Boats. (2012, November). Retracting drive unit [retrieved 13-09-2024]. https://biekerboats.blogspot.com/2012/11/retracting-drive-unit.html

Brans, S. (2021). *Applying a needs analysis to promote daughter craft for year-round access to far-offshore wind turbines* [Master's thesis, Delft University of Technology]. http://resolver.tudelft.nl/uuid:c1de0299-b8f5-42a8-9a0e-71549756f57d

Candela. (2024a, May). https://candela.com/p-12-shuttle/

Candela. (2024b, May). https://candela.com/

Caterpillar. (2024). Marine power solutions [Brochure].

Cauwenberghe, L. V. (2025). *Developing a new hull design for the tenders of 'het loodswezen' to improve the seakeeping behaviour* [Master's thesis, Delft Universisty of Technology]. https://resolver.tudelft.nl/uuid:680b4a5b-7932-4667-9421-ea551a75c738

Cirelli, M., Giannini, O., Cera, M., De Simoni, F., Valentini, P., & Pennestrì, E. (2021). The mechanical efficiency of the rzeppa transmission joint. *Mech. Mach. Theory*, *164*, 104418. https://doi.org/https://doi.org/10.1016/j.mechmachtheory.2021.104418

Deyzen, A. (2013, January). *Improving the operability of planing monohulls sailing in head seas using automated proactive control of the thrust - proof of concept* [Doctoral dissertation, Delft University of Technology].

Doornebos, P., Francis, M., le Poole, J., & Kana, A. (2023). Design and feasibility of a 30- to 40-knot emission-free ferry. *Int. Shipbuild. Prog.*, *70*, 81–114. https://doi.org/10.3233/ISP-230005

Dymarski, C., & Skorek, G. (2006). A design concept of main propulsion system with hydrostatic transmission gear for inland waterways ship. *Pol. Marit. Res.*, *2*, 57–61. https://yadda.icm.edu.pl/baztech/element/bwmeta1.element.baztech-article-BWM3-0007-0025

Edorado. (2024, June). https://edorado.com/

Emirates Team New Zealand. (2022, May). Emirates team new zealand take flight in hydrogen powered foiling chase boat [retrieved 4-10-2024]. https://emirates-team-new-zealand.americascup.com/en/news/549_EMIRATES-TEAM-NEW-ZEALAND-TAKE-FLIGHT-IN-HYDROGEN-POWERED-FOILING-CHASE-BOAT.html

Emrax. (2025). Emrax electric motors/generators [retrieved 28-1-2025]. https://emrax.com/e-motors/

Enata. (2024). Marine [retrieved 31-05-2024]. https://enata.com/marine#marineFoiler

Evolito. (2025). Axial flux motors [retrieved 28-1-2025]. https://evolito.aero/axial-flux-motors/

Faltinsen, O. M. (2005). *Hydrodynamics of high-speed marine vehicles*. Cambridge university press.

Frauenberger, H. C. (1982). Shimrit - mark ii hydrofoil for the israeli navy. *First Int. Hydrofoil Soc. Conf.*, 157–170. https://foils.org/wp-content/uploads/2017/11/0137-IHS-Nova-Scotia-Conference-Papers-Jul-82.pdf

Gabrielli, G., & von Karman, T. (1950). What price speed? *Mech eng.*, *72*, 775–781.

Gelling, J., & Keuning, L. J. (2011). Recent developments in the design of fast ships. *Ciencia y tecnologia de buques*, *5*, 57. https://doi.org/10.25043/19098642.51

German Maritime Museum. (2024). Hydrofoil wss 10 [retrieved 4-10-2024]. https://www.dsm.museum/en/museum/exhibits/hydrofoil-wss-10

Godø, J. M. K. (2024). *Zero-emission hydrofoil fast ferries: Design, modelling, and performance evaluation* [Doctoral dissertation, Norwegian University of Science and Technology]. https://ntnuopen.ntnu.no/ntnu-xmlui/handle/11250/3172953

Godø, J. M. K., Steen, S., & Faltinsen, O. M. (2024). A resistance model for hydrofoil fast ferries with fully submerged foil systems. *Ocean. Eng.*, *301*, 117503. https://doi.org/https://doi.org/10.1016/j.oceaneng.2024.117503

Grevink, J. (2022). Mt44006: Podded propulsors [presentation].

Gurit. (2015, April). Composite technology for work boats - can composites pay their way? https://www.gurit.com/wp-content/uploads/bsk-pdf-manager/2022/08/gurit-delegate-pack-composite-work-boats-fc.pdf

Hoerner, S. (1965). *Fluid-dynamic drag: Practical information on aerodynamic drag and hydrodynamic resistance*. Hoerner Fluid Dynamics. https://books.google.nl/books?id=abU8AAAAIAAJ

Hoerner, S., Michel, W., Ward, L. W., & Buermann, T. M. (1954). *Hydrofoil handbook, hydrodynamic characteristics of components*. Bath Iron Works Corporation By Gibbs; Cox. https://www.foils.org/wp-content/uploads/2018/01/HFhdbkVol_II_1954.pdf

Hosseini, Y. (2024, July). Handling obstacles: Logs and hydrofoil boats [retrieved 25-09-2024]. https://candela.com/handling-obstacles-logs-and-hydrofoil-boats/

Hydrosta. (2024). Hp inline - parallel hybrid propulsion by hydrosta [retrieved 28-1-2025]. https://hydrosta.nl/uploads/documents/FolderHPInLine.pdf

James, T. (2024, August). Spirit bartech f35 launches with acclaim: 100% electric, 100 nautical miles! https://www.bartechnologies.uk/leisure-boats/spiritbartech35ef-launches-with-acclaim/

Johnston, R. J. (1985). Hydrofoils. *Nav. Eng. J.*, *97*(2), 142–199. https://foils.org/wp-content/uploads/2017/12/Naval-Engineers-Journal-Modern-Ships-and-Craft-71242.pdf

Journee, J., Massie, W., & Huijsmans, R. (2015). *Offshore hydromechanics* (Vol. Third edition). Delft University of Technology, Faculteit Civiele Techniek en Geowetenschappen.

Kamp, H. (2021, October). Vervanging en instandhouding frisc (fast raiding, interception and special forces craft) [letter to parliament]. https://www.rijksoverheid.nl/documenten/kamerstukken/2021/10/25/kamerbrief-behoeftestelling-vervanging-en-instandhouding-fast-raiding-interception-and-special-forces-craft

Keuning, L. J. A. (1994, September). *Nonlinear behaviour of fast monohulls in head waves* [Doctoral dissertation, Delft University of Technology]. https://api.semanticscholar.org/CorpusID:118221808

Keuning, L. J., Gerritsma, J., & van Terwisga, P. (1992). *Resistance tests of a series planing hull forms with 30 degrees deadrise angle, and a calculation model based on this and similar systematic series*. Delft University of Technology, Faculty of Mechanical Engineering; Marine Technology. https://books.google.nl/books?id=TE8yAAAACAAJ

Keuning, L. J., & Hillege, L. The results of the delft systematic deadrise series. In: In *Fast2017*. 2017. https://resolver.tudelft.nl/uuid:6ddc5192-107f-47de-8669-38114b9ce16d

Keuning, L. J., & Ligtelijn, D. (2017). High speed craft. *Encycl. Marit. Offshore Eng.* https://doi.org/10.1002/9781118476406.emoe540

Kim, S., & Jeon, H. (2022). Comparative analysis on ac and dc distribution systems for electric propulsion ship. *J. Mar. Sci. Eng.*, *10*(5). https://www.mdpi.com/2077-1312/10/5/559

Klein Woud, J., & Stapersma, D. (2002). *Design of propulsion and electric power generation systems*. IMarEST.

Kossiakoff, A., Biemer, S., Seymour, S., & Flanigan, D. (2020). *Systems engineering principles and practice*. Wiley. https://books.google.nl/books?id=gGzoDwAAQBAJ

Kyunghwa Kim, G. R., Kido Park, & Chun, K. (2018). Dc-grid system for ships: A study of benefits and technical considerations. *J. Int. Marit. Safety, Environ. Aff. Shipp.*, *2*(1), 1–12. https://doi.org/10.1080/25725084.2018.1490239

Lundin, A., & Eriksson, L. (2021). *Concept development and design of a retractable hydrofoil systems* [Master's thesis, Kungliga Tekniska Högskolan] [Dissertation]. https://urn.kb.se/resolve?urn=urn:nbn:se:kth:diva-305446

Man Rollo. (2024). Marine - high speed proulsion engines [Brochure]. https://manrollo.com/wp-content/uploads/Marine_Commercial_220512_web-website.pdf

Mantaray. (2024). Mantaray m25 [retrieved 19-8-2024]. https://www.mantaraycraft.com/m25

Margés, J. (2018). Frisc kent eigen kracht niet. *Alle Hens*, *01*. https://magazines.defensie.nl/allehens/2018/01/00_frisc

McKesson, C. (2014). *The practical design of advanced marine vehicles*. CreateSpace Independent Publishing Platform. https://books.google.nl/books?id=vb-1oAEACAAJ

Mewis, F. (2002). The efficiency of pod propulsion. *HADMAR 2001*. https://api.semanticscholar.org/CorpusID:209898546

Minerva, L., & Montero, F. (2021). Experimental investigations on conventional and unconventional boost systems to assist take-off of hydrofoil crafts. *7th High Perform. Yacht Des. Conf. 2021*. https://www.proceedings.com/content/058/058917webtoc.pdf

Minerva, L. F., Odendaal, K., Marelli, G., & Scholcz, T. (2024). Early design of hydrofoils: Foil design jip overview and methods. *28th Int. HISWA Symp.* https://hiswasymposium.com/wp-content/uploads/HISWA-2024-Early-Design-of-Hydrofoils_Foil-Design-JIP-overview-and-methods_Minerva-Odendaal-Marelli-Scholcz.pdf

Mørch, J. (1992). *Aspect of hydrofoil design with emphasis on hydrofoil interaction in calm water, dr. ing* [Doctoral dissertation, Department of Marine Hydrodynamics, NTNU, Trondheim, Norway].

Navier. (2024). N30 - the boat of the future [retrieved 19-8-2024]. https://www.navierboat.com/

Netherlands Ministry of Defence. (2023, November). European tendering procedure for the delivery of littoral assault craft including associated goods and services.

Netherlands Ministry of Defense. (n.d.). Lcvp-landingsvaartuig (personeel) [Licensed under CC BY-SA 4.0]. https://www.defensie.nl/onderwerpen/materieel/schepen/lcvp-landingsvaartuig-personeel

Newton, R., & Rader, H. (1961). Performance data of propellers for high-speed craft. *The Royal Inst. Nav. Archit.*, *103*(2).

Oh, D., Jung, S., & Jeong, S. (2018). Effect of a Lightweight Hull Material and an Electric Propulsion System on Weight Reduction: Application to a 45ft CFRP Electric Yacht. *J. Korean Soc. Mar. Environ. Saf.*, *24*, 818–824. http://www.kosomes.or.kr/journalarticle.php?code=64534

Olofsson, K., Arnestad, G., Lönnö, A., Hedlund-Åström, A., Jansson, T., & Hjortberg, M. (2008). A high-speed craft with composite hull. *Proc. 13th Eur. Conf. Compos. Mater.*

Peek, R., & Bauer, L. (1981). M151 transmission for mark ii hydrofoils. *AIAA 6th Mar. Syst. Conf.*, (81-2084). https://foils.org/m-151-transmission-for-mark-ii-hydrofoils/

Pugh, S. (1991). *Total design : Integrated methods for successful product engineering*. Addison-Wesley Pub. Co. http://books.google.com/books?id=RKIQAQAAMAAJ

Rolls-Royce. (2024). M250/rr300 - 2024 first network directory [retrieved 28-1-2025]. https://www.rolls-royce.com/products-and-services/civil-aerospace/helicopters/m250-turboshaft.aspx#section-training

Saab. (2021). Cb90 next generation at a glance [retrieved 20-6-2024]. https://www.saab.com/contentassets/e40e2f9b6b3b4c1f8e4b86080dc36111/cb90-ng-at-a-glance.pdf

Savitsky, D. (1964). Hydrodynamic Design of Planing Hulls. *Mar. Technol. SNAME News*, *1*(04), 71–95. https://doi.org/10.5957/mt1.1964.1.4.71

Scania. (2024). Di16 077m. 662 kw (900 hp) [retrieved 30-8-2024]. https://www.scania.com/content/dam/scanianoe/market/master/products-and-services/engines/pdf/specs/marine/DI16077M_662kW.pdf

Scania. (2025). Specifications of maritime energy systems [retrieved 28-1-2025]. https://www.scania.com/nl/nl/home/products/power-solutions/marine-power-systems/marine-power-systems-specifications.html

SEAir solutions. (2024). https://seair-solutions.com/

Ship Motion Group. (2024). Retractable propulsion system [Brochure].

Stam, M. (2025). *Modular naval vessels and the impact on the design and effectiveness* [Master's thesis, Delft University of Technology]. Modular%20naval%20vessels%20and%20the%20impact%20on%20the%20design%20and%20effectiveness

Stenius, I., Rosén, A., & Kuttenkeuler, J. (2011). On structural design of energy efficient small high-speed craft. *Mar. Struct.*, *24*(1), 43–59. https://doi.org/https://doi.org/10.1016/j.marstruc.2011.01.001

Streng, J., Kana, A., Verbaan, J., Barendregt, I., & Hopman, J. (2022). Alternative energy carriers in naval vessels. *Int. Nav. Eng. Conf.*

Strijbosch, V. (2019). De marine in 2035. *Alle Hens*, (4). https://magazines.defensie.nl/allehens/2019/03/05_doctrine

Trancossi, M. (2016). What price of speed? A critical revision through constructal optimization of transport modes. *Int. J. Energy Environ. Eng.*, *7*(4), 425–448. https://doi.org/10.1007/s40095-015-0160-6

Tyde. (2024). The icon [retrieved 26-09-2024]. https://tyde.one/the-icon-2

van Oossanen, P. (1983). Geavanceerde scheepstypen (in dutch). *Schip en Werf*, *50*(4), 43–59.

van Walree, F. (1998). *Hydres manual*.

van Walree, F. (1999). *Computational methods for hydrofoil craft in steady and unsteady flow* [Doctoral dissertation, Delft University of Technology]. %7Bhttp://resolver.tudelft.nl/uuid:3bb919b0-7eab-443d-a498-b58c896a7498%7D

van Walree, F. (2002). Development, validation and application of a time domain seakeeping method for high speed craft with a ride control system. *24th Symp. on Nav. Hydrodyn.* https://www.marin.nl/en/publications/development-validation-and-application-of-a-time-domain-seakeeping-method-for-high-speed-craft-with-a-ride-control-system

van Walree, F. (2015, November). *Panship developments for fast ship simulation* (tech. rep.). MARIN. https://www.marin.nl/en/publications/panship-developments-for-fast-ship-simulation

van Walree, F. (2025, February 20).

van den Bosch, J. (1970). *Tests with two planing boat models in waves* (tech. rep.). Delft University of technology. https://repository.tudelft.nl/record/uuid:02d190b3-7646-4228-a5ca-64c93820c1cc

van der Maat, C. (2023, March). Vervanging middelzwaar landingsvaartuig (lcvp) [letter to parliament]. https://www.rijksoverheid.nl/documenten/kamerstukken/2023/03/22/kamerbrief-a-brief-over-project-vervanging-middelzwaar-landingsvaartuig-lcvp

van der Maat, C. (2024, March). Verwerving amfibische transportschepen [letter to parliament]. https://www.rijksoverheid.nl/documenten/kamerstukken/2024/03/07/kamerbrief-a-brief-project-verwerving-amfibische-transportschepen

Vessev. (2024). Vs-9 [retrieved 13-8-2024]. https://www.vessev.com/

Volvo Penta. (2025). All marine engines [retrieved 28-1-2025]. https://www.volvopenta.com/marine/all-marine-engines/

Wartzack, S. (2021). *Technical pocket guide*. Schaeffler Technologies AG & Co. KG.

Yanmar. (2025). Commercial high speed diesel engines [Brochure]. https://www.yanmarmarine.eu/theme/yanmarportal/uploadedFiles/Marine/productDownloads/Commercial-Product-Guide/100x210_Brochure_CHS_Marine_Product_handbook__nieuwlogoLRforweb.pdf

Yun, L., & Bliault, A. (2014). *High performance marine vessels*. Springer New York. https://books.google.nl/books?id=3wcDzNJpXf0C

Zwinkels, R. M. (2025, April). *Operational effectiveness of hydrofoils for littoral craft* [Master's thesis, Delft University of Technology]. https://resolver.tudelft.nl/uuid:0c4647f2-f817-4cd0-ba49-e4c9638a6778